Serviceability of plate heat exchanger gaskets bonded with various adhesives

Daniel Perucho Barichevskaia

Department of Physics, Division of Solid State Physics
Faculty of Science | LUND UNIVERSITY
Supervised by Jens Rassmus and Pablo Villanueva Pérez
Project Duration: 30 ECTS, 4 months full-time equivalent
Date of examination: June 2026
Project duration: 4 months (full-time equivalent)
Master Programme in Materials Science - Physics

MASTER'S THESIS

Acknowledgements

First of all, I would like to express my sincerest gratitude to Jens Rassmus for giving me the opportunity to carry out this thesis. His support and motivation have been fundamental throughout the development of this project, not only because of his valuable perspective from the field of materials science, but also for encouraging a healthy and consistent work ethic. He was always highly receptive to my ideas, no matter how ambitious they initially seemed, and continuously did everything possible to help me put them into practice. I am also deeply grateful for all the valuable feedback and the unconditional support he provided from the very beginning of this thesis.

I would also like to make a special mention to Emina Kujundzic for co-supervising this project. She has been an exceptional mentor throughout this project. Thank you for all the guidance and support received in the laboratory, always prioritizing safety and patiently teaching how experimental work should be properly conducted, while constantly providing a valuable perspective. Special thanks to the staff at the service center in Staffanstorp for their support during the experimental work and for giving me access to their equipment and facilities.

In addition, I would like to thank Pablo Villanueva for his valuable feedback and helpful suggestions throughout this thesis.

More generally, I would like to express my sincere gratitude to all the employees at Alfa Laval, especially the Research and Development team, for making me feel welcome from the very first day and for integrating me as part of the team. I am deeply grateful for the valuable experience gained during my time at Alfa Laval.

Last but not least, I would like to thank my family for their unconditional support throughout my journey as a physicist, for supporting my decision to move to Sweden to pursue a Master's degree, and for always believing in the value of my education. Thanks to them, I have been able to begin a new chapter of my life in Sweden, a country that will always hold a special place in my heart. I also want to express my sincere gratitude to my family and friends for their continuous encouragement and support. None of this would have been possible without them.

Abstract

Plate heat exchangers are widely used in industry due to their high thermal efficiency and versatility, compact design and ease of maintenance. In gasketed plate heat exchangers (GPHEs), the reliability of the system strongly depends on the adhesion between the elastomeric gasket and the metallic plate.

Although GPHEs can be periodically opened and cleaned to restore heat transfer efficiency, cleaning procedures based on high-pressure water jetting may progressively weaken adhesive interfaces and compromise the gasket serviceability. The durability of these bonded systems is governed by complex interfacial phenomena involving adhesion mechanisms, polymer crosslinking, moisture diffusion and crack propagation. However, the relationship between adhesive bond strength and gasket survival during industrial cleaning operations remains poorly understood.

This study demonstrates that peel testing is an effective method for characterizing the adhesion performance of gasket–adhesive–metal systems and assessing their serviceability under high-pressure water jetting conditions. Different systems based on NBR and EPDM gaskets together with several industrial adhesives were investigated through peel testing, water jetting experiments and SEM-EDS analysis. The results reveal a clear correlation between the critical peeling force and the resistance of the gasket to detachment during water jetting. Systems with low bond strength detached easily during water jetting, whereas high-strength epoxy-based systems remained intact under the investigated cleaning conditions.

These findings demonstrate that peel testing and water jetting are strongly interconnected and together provide a comprehensive description of gasket serviceability. The study also highlights the importance of curing conditions, adhesive-gasket compatibility and gasket polarity in determining adhesion performance and interfacial degradation. Furthermore, experimentally determined critical force thresholds are proposed, establishing practical limits for the cleaning conditions under which adhesively bonded gaskets can safely operate.

Keywords: Gasketed plate heat exchangers (GPHE), Adhesion, Epoxy adhesives, Elastomeric gaskets, NBR, EPDM, Peel testing, Water jetting, Serviceability, Interfacial fracture, Ageing, SEM-EDS.

Popular Science Writing

Imagine a factory, a power plant or even the heater of your own flat stopped working. The reason? A tiny rubber gasket that has come loose. It might sound like a joke but behind that small piece lies a fascinating science and major industrial challenge. This master's thesis dives into this invisible and little-known world: how and why adhesives hold critical components together and what happens when we use them for one of the most common devices in the world, plate heat exchangers. Adhesively bonded gaskets are the unknown heroes of plate heat exchangers, devices essential to industry and daily life. They allow two liquids to exchange heat without mixing, making them suitable for all kinds of applications, from building climate control to food production. At the heart of these exchangers are dozens of metal plates, each with a rubber gasket glued along its edge, preventing leakage and ensuring a good sealing. If even one gasket fails, the system can lose efficiency, contaminate fluids, or even break down entirely.

But why not just weld the plates together? The answer is rather uninspiring, but it is the reality. Over time, especially when seawater is involved, plates can become clogged and need to be cleaned in order to restore its efficiency. Adhesively bonded gaskets, unlike welded heat exchangers, allow the system to be opened and cleaned, but this exposes the adhesive joints to mechanical and thermal stresses that can compromise the bond. Here is the challenge: how do we ensure these gaskets keep working after repeated cleanings?

Sticking two materials together might seem simple, but the science behind adhesion is surprisingly complex. There is not a single theory that explains why adhesives work, in fact, it is a combination of all of them: mechanical interlocking, electrical forces, chemical reactions, diffusion and more. This research focuses on how these mechanisms operate between the metal plate and the rubber gasket and how different adhesives respond to the stresses of industrial cleaning.

During my thesis in Alfa Laval, a world leader company in heat exchangers, I studied two types of rubber: NBR and EPDM. Each has unique chemical properties, which affect how well they bond with adhesives and how durable that bond is. The result? A wide range of adhesive-gasket combinations, all of which need to be tested under extreme conditions to find out which ones stand after cleaning. In order to test these bonds I subjected the gaskets to peel testing experiments combined with high-pressure water jets, simulating the industrial cleaning process. Then, I analyzed how and where the bonds failed. The goal is clear: to understand which adhesives and materials offer the greatest durability, and to set safe limits for cleaning procedures.

This project is not just about solving an industrial problem, it also contributes to a scientific field full of unanswered questions. Adhesion is fundamental to countless applications, from medicine to space exploration. Every step forward in understanding these mechanisms can help to improve the efficiency, safety and serviceability of technologies we rely on every day.

This thesis is a small step toward a world where machines run better and longer, thanks to a science as invisible as it is essential: the glue that holds everything together.

Contents

1 Introduction

Plate heat exchangers are essential components in a wide range of industrial processes and everyday applications, enabling the efficient transfer of thermal energy between fluids without mixing them. The integrity and serviceability of these devices depend largely on the performance of their gaskets, which are rubber-made components located at the ends of the plates that ensure leak-free operation under varying thermal and mechanical loads. This thesis was conducted in collaboration with Alfa Laval, a world-leading manufacturer of plate heat exchangers specialized in the production of adhesively bonded gasketed plate heat exchangers (GPHE). This variant of plate heat exchangers is currently the most versatile and best suited to the customer's needs, representing a large proportion of the company's sales. This is not only due to their excellent sealing reliability, high assembly efficiency and large volume capacity compared to welded plate heat exchangers, but also because they offer maintenance opportunities that are unimaginable for their welded counterparts. [1]

One external factor that must be considered in the maintenance of these devices is clogging. After prolonged use, especially when seawater is involved, the plates may become clogged, significantly reducing the heat transfer efficiency. In such cases, GPHEs offer the major advantage that they can be opened and cleaned periodically. Consequently, high heat transfer efficiency can be restored easily and cheaply without the need to purchase a new plate heat exchanger. However, during the cleaning process, both mechanical and thermal stresses are exerted on the adhesive joints, potentially leading to a reduction in adhesion. [1]

Despite the critical role of adhesive bonded gaskets in plate heat exchangers, significant scientific challenges remain in predicting and optimizing their service. Specifically, there is a lack of data regarding the adhesive bond strength required to withstand a high-pressure water jetting. This thesis will investigate the serviceability of adhesively bonded gaskets under cleaning conditions, aiming to analyze and quantify the influence of cleaning parameters on adhesive bond strength, compare the performance of different epoxy-based adhesives under such conditions and determine operational thresholds for cleaning parameters to ensure gasket serviceability.

The fundamental challenges addressed in this work are rooted in materials science, particularly the study of interfacial phenomena which involves considerations of chemical compatibility, thermal stability, mechanical resilience and of course the explanation behind the interfacial adhesion between the gasket material and the metallic plate substrate. The approach adopted to address these challenges is based on a extensive literature review, combined with a range of experimental tests and material characterization techniques, with the aim of quantifying and optimizing the performance of adhesive bonded joints.

2 Gasketed Plate Heat Exchangers (GPHE)

Alfa Laval is a company whose main product is plate heat exchangers. There are many types of plate heat exchangers, which differ mainly in how they seal the fluid between adjacent plates. Adjacent plates can be brazed, welded or use gaskets, which can be secured with clips (mechanically attached) or bonded with adhesive. [1] This project will study the glue bonded gasketed plate heat exchangers.

2.1 Design

Gasketed plate heat exchangers (GPHE) are a class of compact heat exchangers characterized by their modular construction and high thermal efficiency. These devices consist of a series of thin, corrugated metal plates arranged in parallel and compressed together in such a way that there are very narrow flow channels between adjacent plates, where the heat exchange fluid circulates. The plates are typically fabricated from stainless steel, titanium or other corrosion-resistant alloys, chosen for their malleability combined with a high thermal conductivity and mechanical strength. [2]

The primary function of a GPHE is to facilitate the heat transfer of two fluid streams without allowing direct contact between them. This is achieved by creating a large surface area for heat exchange within a compact space and using the corrugations on the plates to create a turbulent flow. The more turbulence, the better and more efficient the heat transfer between plates will be. [3] Along the edges of each plate there is a groove marking where the gasket is located, which is adhesively bonded to the plate. These adhesively bonded gaskets are crucial for the operation of the heat exchangers and will be the main focus of this project as they are responsible to ensure sealing, durability and serviceability, but also to define the flow configuration such as counterflow, parallel flow or crossflow; which influences the heat exchanger's thermal performance and pressure drop characteristics. Below is shown an example of a gasketed plate from a GPHE:

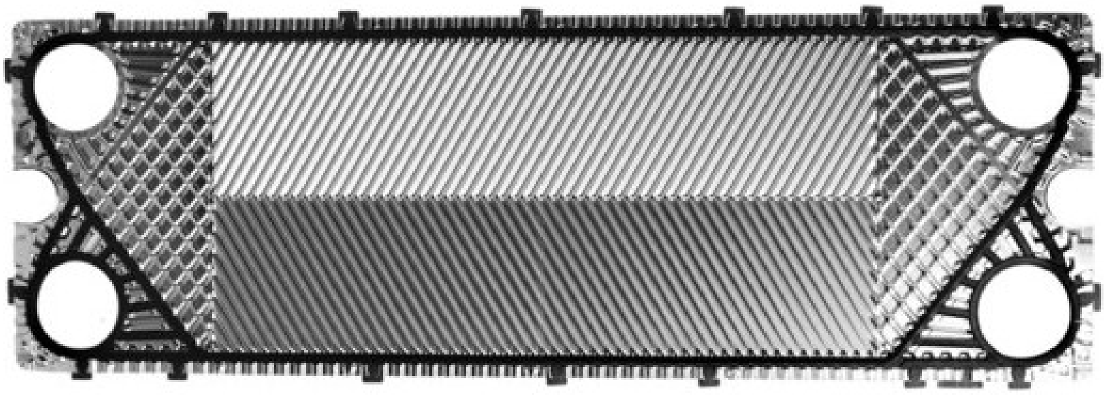

Figure 1: Picture of a gasketed plate used in a GPHE. The component consists of a stainless steel plate with a corrugated pattern designed to enhance flow turbulence and heat transfer efficiency, together with a groove where the gasket is positioned and protected during operation. [4]

2.2 Working principle and applications

Plate heat exchangers are the most thermally efficient type of heat exchanger, far surpassing traditional shell-and-tube heat exchangers. [1] Their working principle is illustrated in Figure 2. It consists of a system with two inputs (a hot liquid and a cold liquid) and two outputs (the cooled hot liquid and the heated cold liquid). A frame holds all the plates in place and distributes the liquids through the corresponding inlet and outlet ports. In order to optimize heat exchange between the fluids, they are distributed as follows: a hot fluid and a cold fluid flow alternately and in opposite directions between the plates. Thanks to the design of the gaskets and plates, the fluids do not mix and flow with high turbulence, further enhancing heat exchange. [2] [5]

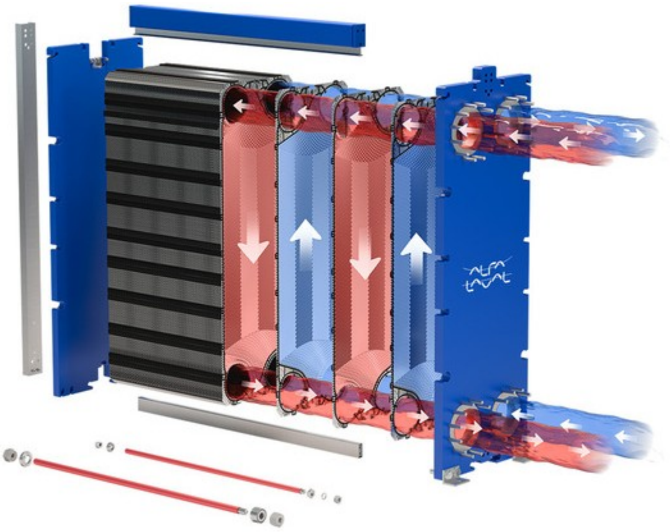

Figure 2: Plate heat exchanger working principle. Two fluids at different temperatures exchange heat without mixing. [4]

Despite its simple working principal, GPHEs are essential in multiple industries, especially where it requires a frequent maintenance, cleaning and operational flexibility. For example, in dairy processing plants GPHEs are used to pasteurize milk by rapidly heating and cooling it, ensuring both product safety and energy efficiency. In marine applications such as ships, GPHEs are used to cool engine lubricants in order to maintain optimal engine performance and prevent overheating. In power generation such as nuclear reactors, GPHEs are employed to cool the reactor water or turbine lubricants. Furthermore, it covers not only industrial needs but it can also be used in everyday life situations. For instance, GPHEs are commonly found in residential buildings that have a shared heating infrastructure, where these heat exchangers transfer heat from a central boiler or a district heating network to the building's internal heating circuit. This allows each apartment to receive hot water for radiators or domestic use, while keeping water circuits separate for safety and efficiency. [6]

Compared to welded or brazed plate heat exchangers, gasketed designs offer significant advantages, specially in terms of versatility and adaptability to the customer's needs. [2] Welded and brazed exchangers are typically used in applications where high pressure or aggressive fluids are present, but their sealed construction makes them difficult or impossible to open for cleaning or inspection, which makes them vulnerable to some loss of efficiency. [7] In contrast, gasketed plate heat exchangers can be easily disassembled, allowing operators to remove fouling and restore the heat transfer efficiency, replace gaskets or adjust capacity by adding or removing plates. This modularity is particularly valuable in sectors like food and drink industry, where hygiene standards require regular cleaning, or in situations in which seawater is used since it promotes the formation of bio-fouling, which significantly reduces the efficiency of heat transfer. [1]

The main difference between glue bonded gaskets and mechanically fastened gaskets in GPHEs lies in their attachment method and, as a consequence, their durability. The gaskets that are mechanically attached to the plate are more susceptible to come loose during operation or in the cleaning process. In contrast, glue bonded gaskets are chemically attached to the plate due to the hardening of the adhesive, providing a more secure and permanent attachment that resists loosening, even under repeated cleaning cycles. This enhanced stability, which improves the reliability and service life of the heat exchanger, in addition to a great flexibility and maintainability, make the glue bonded GPHEs the preferred choice. [2]

2.3 Cleaning process

In case of a customer notices an efficiency drop in a GPHE due to the accumulation of fouling and clogging inside the plates, a standardized maintenance protocol is initiated. The first step typically involves cleaning the unit either with a caustic-based solution to remove bio-fouling or an acid-based solution if it is inorganic clogging. If this treatment does not fully restore performance and there is significant fouling remaining, the heat exchanger is disassembled and subjected to high-pressure water jet cleaning. In cases where fouling persists even after these actions, the unit may be sent to an Alfa Laval service center, where the plates undergo an intense cleaning using a combination of caustic and acid baths, accompanied by water jetting. [8]

Throughout these cleaning procedures, especially during the high-pressure water jetting, the gaskets are repeatedly exposed to harsh chemical and mechanical stresses, making them particularly vulnerable to debonding or damage. Currently, Alfa Laval lacks comprehensive data regarding the adhesive bond strength required to withstand a high-pressure water jetting, as well as the specific conditions (such as spraying angle, distance nozzle-gasket and cleaning parameters) that most influence gasket detachment. Furthermore, it remains unclear which cleaning methods best preserve gasket integrity and extend service life. Overall, there is a need that this thesis aims to solve in determining the serviceability of adhesively bonded gaskets in gasketed plate heat exchangers.

3 Adhesives

The use of adhesives has revolutionised modern industry, enabling the fabrication of lighter and more efficient products with an improved design. The case of gasketed plate heat exchangers is not an exception as adhesives play a crucial role in their assembly and performance, being responsible for maintaining the integrity of the seal between the gasket material and the metallic plate. Their behaviour under mechanical loads, temperature variations and chemical exposure directly influences the serviceability and durability of the bonded joint. [6]

Adhesives can be defined as a material which when applied to surfaces of materials can join them together and resist separation. [9] Unlike other joining methods, such as welding or bolting, adhesives allow similar or dissimilar materials to be joined without significantly altering their structure or integrity. From a physical point of view, an adhesive can be defined as a material which, when applied in a liquid state, develops cohesive and adhesive properties as it cures, enabling the transfer of loads between the joined substrates. Adhesive forces are responsible for the adhesion at the interface, between the adhesive and the substrates; and cohesive forces act within bulk of the adhesive, which means that they are responsible for maintaining a consistent and rigid structure within the adhesive itself. [10]

3.1 Properties of adhesives

The main component of an adhesive is an organic polymer, or one or more compounds that can chemically react to produce a polymer. [9] However, even though all adhesives share a polymeric basis, they can exhibit a wide variety of properties and can be classified in different ways. The most common types include epoxy, acrylic, polyurethane, cyanoacrylate and hot-melt adhesives. Each has specific characteristics in terms of strength, flexibility, curing time and compatibility with different materials. If we distinguish them based on their curing process and structure, we find two types:

- **Thermoplastics:** Thermoplastic adhesives consist of polymer chains that are not chemically crosslinked. As a result, they soften when heated and solidify when cooled, so their curing process is reversible. Their bonding mechanism is primarily based on physical interactions and they generally exhibit good flexibility but limited mechanical strength and thermal resistance. An example of a thermoplastic adhesive is hot-melt adhesive. [10]
- **Thermosets:** Thermosetting adhesives experience an irreversible chemical reaction during curing, leading to the formation of a three-dimensional crosslinked network. This structure provides high mechanical strength, thermal stability and chemical resistance, making thermosetting adhesives particularly suitable for demanding applications that require a strong adhesive. Some adhesive families that are thermosetting adhesives are epoxy, acrylic, polyurethane and cyanoacrylate adhesives. It should be noted that acrylics and polyurethanes can be formulated as either thermoplastic or thermosetting systems depending on their curing chemistry and degree of crosslinking. [10]

In short, crosslinking is the key process that distinguishes thermosetting adhesives from thermoplastic systems. Crosslinking consists on the formation of covalent bonds between polymer chains during the curing process, which translates into the development of a three dimensional network structure reducing the molecular motion. As the degree of crosslinking increases, the material transitions from a viscous or semi-liquid state to a rigid solid that cannot be remelted or reshaped. The degree or extent of crosslinking can be described by the crosslink density, a key parameter that might greatly affect the properties of the adhesive and mainly depend on the curing method. [11] A high crosslink density generally results in increased stiffness, strength and resistance to solvents and elevated temperatures. However, it also reduces the material's ability to deform, making it more brittle. On the other hand, a lower crosslink density results in a more flexible and tougher material but with reduced mechanical and thermal resistance. [10] Therefore, two samples with same adhesives (in terms of composition) but different curing methods, which translates to a difference in crosslink density, can result in two completely different adhesives in terms of performance. It is not only the chemical composition of the adhesive that matters, but also the curing conditions which determine the crosslink density. The optimization of crosslinking density is not an easy task since it is a trade-off between mechanical strength and toughness, which is particularly relevant for gasket applications subjected to cyclic mechanical and thermal loads.

In the case of epoxy-based adhesives, crosslinking typically occurs through a reaction between epoxide groups and curing agents such as amines that are in hardeners, resulting in a highly interconnected network. This network structure restricts molecular mobility, which is directly responsible for the high mechanical strength, thermal stability and chemical resistance characteristic of thermosetting systems. [9] In order to better understand the crosslinking process of epoxy-based adhesives, a diagram is shown in Figure 3.

From a serviceability point of view, crosslinking plays a crucial role in determining the durability of adhesive joints under cleaning conditions. Exposure to heat, humidity, or aggressive chemicals can alter the network structure through mechanisms such as chain scission, plasticization or hydrolysis. [11] These effects may reduce the effective crosslink density, leading to a deterioration of mechanical properties and adhesion performance; a process which will be referred to in this thesis as “ageing”.

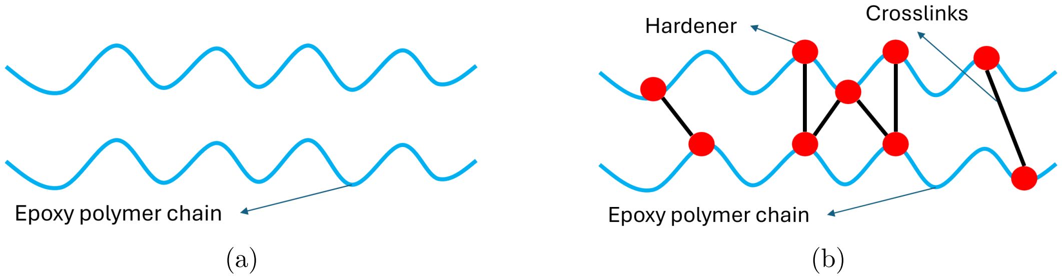

(a) (b)

Figure 3: Epoxide polymer chains (in blue) before (a) and after (b) the crosslinking process. When an epoxide is mixed with a hardener (in red) such as amines, there is a chemical reaction which results in the formation of new covalent bonds named crosslinks (in black) between polymer chains.

The glass transition temperature (T_g) is another fundamental property of polymeric adhesives that defines the temperature range over which the material transitions from a rigid and glassy state to a more flexible and rubbery state. Contrary to melting, this transition does not involve a phase change, but instead a significant increase in molecular mobility within the polymer network. For temperatures below T_g, the polymer chains are highly restricted, resulting in a stiff and brittle material with high elastic modulus. Above T_g, the chain mobility increases, allowing a greater deformation and a softer behaviour. This transition has a direct impact on the mechanical performance of adhesive joints. [10]

In thermosetting adhesives such as epoxies, the glass transition temperature is strongly influenced by the crosslink density of the network. A high degree of crosslinking restricts molecular motion and shifts T_g to higher temperatures. [11] From a serviceability point of view, T_g is a critical parameter for determining the operating limits of adhesive bonds. If the working temperature approaches or exceeds T_g, the adhesive may experience a significant reduction in stiffness and strength, which could lead to the failure of the bonded joint. Therefore, ensuring that both the operating and cleaning temperatures remain sufficiently below the glass transition temperature is essential to maintain the structural integrity of adhesively bonded gaskets.

3.2 Adhesives in Alfa Laval

At Alfa Laval there are multiple adhesives that are used depending on the applications and uses of the GPHEs. All the glues used during the thesis are presented below:

- **GC5**: the GC5 adhesive is a one component adhesive sealant that cures upon exposure to atmospheric moisture in room temperature, forming a resilient and flexible silicon rubber. Its bond strength is very weak but it counts with the advantage to be approved by the FDA, which means that this adhesive can be used for food applications (it is eatable). As most of the silicone adhesives, GC5 is a thermoset sealant, which means that despite its rubber appearance, it cannot be softened when heated. The hardening process does not involve any hardener, it cures with humidity from the air. [12]

- **GC6**: the GC6 adhesive is a mixture of two adhesives named GC6B and GC6C. The first adhesive (GC6B) is an epoxy resin and the second one (known as GC6C) is based on a phenol-formaldehyde resin. This mixture is cured in an oven, resulting in an oven-cured adhesive that combines the best properties of each resin: the high strength of the epoxy resin and the flexibility of the phenolic resin. Both phenol-formaldehyde and epoxy resins are classic thermosets which cure by a chemical reaction as represented in Figure 3, forming a rigid and irreversible network. [13]

- **GC8**: the GC8 adhesive is an acrylic nitrile/phenol resin that cures by crosslinking as the solvent evaporates at room temperature. The hardening occurs as the solvent evaporates, triggering a chemical crosslinking reaction that forms a rigid, irreversible structure. Although it is a thermosetting adhesive, there is no hardener, instead, it cures by crosslinking when the solvent starts evaporating. [14]

- **GC11**: the GC11 adhesive is a two component epoxy based on a toughened epoxy resin and an amine hardener. The epoxy resin reacts with the amine hardener at room temperature forming a strong, crosslinked network that, once cured, it cannot be softened by heat (since it is a thermoset). It cures very rapidly compared to the rest of the adhesives, making its handling very quick. [15]

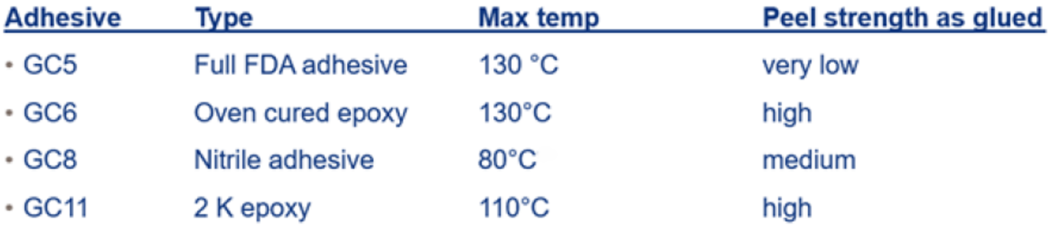

Adhesive	Type	Max temp	Peel strength as glued
• GC5	Full FDA adhesive	130 °C	very low
• GC6	Oven cured epoxy	130°C	high
• GC8	Nitrile adhesive	80°C	medium
• GC11	2 K epoxy	110°C	high

Figure 4: Table summarizing the four adhesives that have been used during the thesis, their type, maximum working temperature and peel strength. [16]

4 Theories of adhesion

From a materials science perspective, the performance of an adhesive bonding is determined by both interfacial interactions and the intrinsic properties of the adhesive itself. [10] Therefore, understanding the basic principles of adhesion is essential before analyzing their behaviour under service and cleaning conditions.

However, despite the phenomenon has been widely studied and described by several complementary theories, each focusing on different physical and chemical phenomena occurring at the interface between the adhesive and the substrate; no single theory is capable to fully explain the adhesion mechanism in all systems.

The most accepted view is that the adhesive bonding cannot be attributed to a unique-mechanism. In fact, it is a combination of multiple mechanisms acting simultaneously that makes adhesion possible. [17] The most commonly accepted theories include mechanical interlocking, thermodynamic theory, diffusion, electrostatic interactions, chemical bonding and intermolecular forces, and weak boundary layer. The relative contribution of each mechanism depends strongly on the nature of the adherends and adhesive involved, the surface properties and the processing conditions. [10]

4.1 Mechanical interlocking

Mechanical interlocking is one of the earliest proposed mechanisms to explain adhesion and is based on the physical anchoring of the adhesive into the microscopic irregularities of the substrate surface. This theory states that when a liquid adhesive is applied, it can flow into irregularities and pores that are on the surface resulting from roughness or porosity; as it cures, it solidifies and forms a mechanical "lock" that prevents separation as shown in Figure 5. [18]

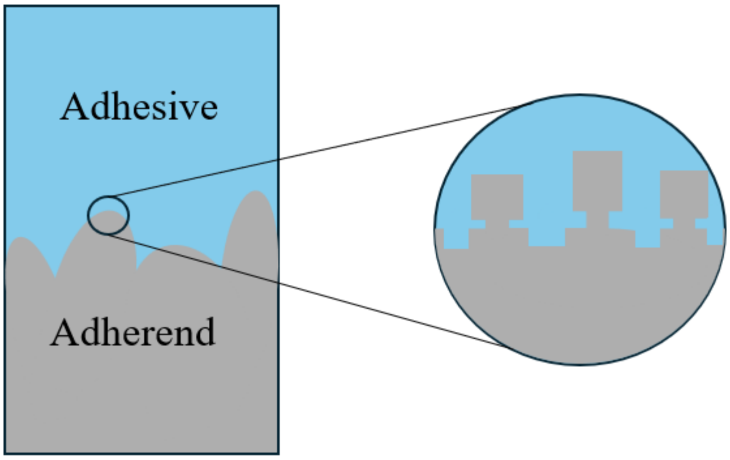

Figure 5: Diagram explaining the mechanical interlocking between the adherend and the adhesive. Due to the surface roughness and porosity of the adherend (in gray), the adhesive (in blue) gets physically anchored after hardening.

The effectiveness of this mechanism depends strongly on the surface roughness and the ability of the adhesive to properly wet the substrate prior to curing. [17] Adequate wetting is essential to ensure that the adhesive penetrates into surface features, maximizing the contact area and the degree of interlocking. This explanation applies quite good in most of the cases but it cannot be the only mechanism behind adhesion since it has been shown that even adherends with perfectly smooth surfaces can form strong bonds. [18]

4.2 Thermodynamic theory

The thermodynamic theory of adhesion is based on the principle that adhesion occurs when the formation of an interface between two materials results in a reduction of the overall free energy of the system. This theory argues that the bond strength of the system is directly related to the adhesive's ability to maintain continuous contact with the substrate, promoting intimate molecular contact with the adherend, a property known as wettability. Wetting is a very important factor since it determines how close the molecules of the bonded materials can get. Therefore, by ensuring good wetting, reduced interfacial distances are achieved, resulting in strong adhesive forces acting on the system. [18]

The degree of wetting depends mainly on the surface energy of both the adhesive and the adherend. Surface energy, denoted by γ, is defined as the energy required to create a new surface per unit area. In a solid–liquid–vapor system the relation of surface and interfacial energies is given by the Young's equation [19]:

$$\gamma_{sv} = \gamma_{sl} + \gamma_{lv} cos(\theta) \tag{1}$$

Where subscripts refer sv to solid-vapour interface, sl to solid-liquid interface and lv to liquid-vapour interface. In addition, there is a dependency on the contact angle θ. This parameter is not an intrinsic property of either the liquid or the solid alone, but rather a result of the energetic equilibrium of the system. A small contact angle indicates good wetting, meaning that the adhesive spreads easily and maximizes the interfacial contact area; whereas a large contact angle corresponds to poor wetting and limited contact, reflecting a poor affinity between the liquid and the solid. [18] For a better understanding of the Young's equation a diagram is shown in Figure 6.

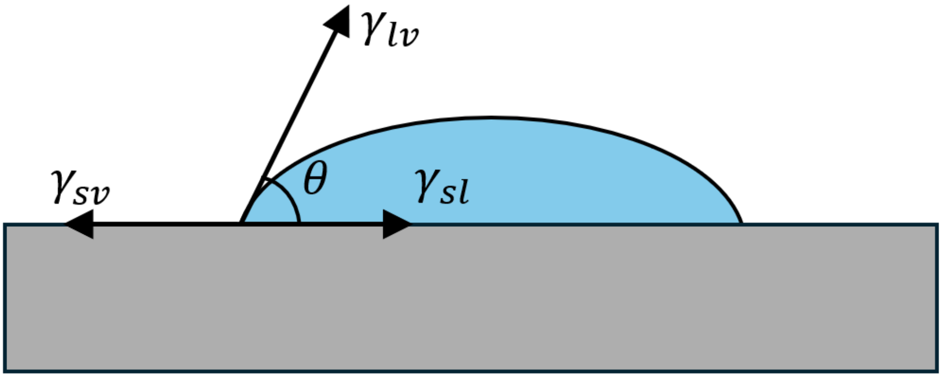

Figure 6: Diagram explaining the contact angle (θ) and tensions (γ) for a liquid drop (in blue) on a solid surface (in gray).

On the other hand, the work of adhesion W_A is defined as the energy required to separate reversibly a unit area of a solid–liquid interface into a free solid surface and a free liquid surface. From an energetic point of view, this process is described by Dupré's equation [19]:

$$W_A = \gamma_s + \gamma_l - \gamma_{sl} \tag{2}$$

If both Equations (1) and (2) are combined and assuming that the surface energy component with the vapour can be neglected ($\gamma_{sv} \simeq \gamma_s$ and $\gamma_{lv} \simeq \gamma_l$), the work of adhesion can be expressed in terms of measurable parameters:

$$W_A \simeq \gamma_l(1 + cos(\theta)) \tag{3}$$

This expression, known as the Dupré–Young equation, shows that the work of adhesion is maximum for small contact angles ($\theta = 0°$ is the ideal case) and liquids with a high energy surface. The greater is the work of a adhesion the greater the wettability of the adhesive on the substrate. [20] However, in order to optimize the work of adhesion, it is necessary to find a balance between the surface energy of the liquid and the contact angle. An increase in γ_l corresponds to an increase in the contact angle and viceversa. Hence, the optimization of wetting is not straightforward. For a fixed rubber and metal combination, maximizing bond strength based solely on wettability is not achieved by optimizing the surface energy of the adhesive, but rather by matching it appropriately to the surface energies and chemical nature of both substrates. A good wetting is a necessary but not a sufficient condition for adhesion.

Although wetting is only one of the mechanisms responsible for adhesion, it describes the quality of interfacial contact and constitute a necessary condition for the development of a strong adhesive bond. [10]

4.3 Electrostatic theory

The electrostatic theory of adhesion proposes that adhesive bonding is based on the formation of an electrical double layer at the interface between the adhesive and the substrate. According to this theory, when two materials with different electronic properties come into contact, there is a transfer of electrons across the interface. As a result, as shown in Figure 7, there is a development of opposite charges on each side, creating regions with a positive (δ^+) and negative (δ^-) partial charge on both surfaces, developing an attractive electrostatic force that contributes to adhesion. [20]

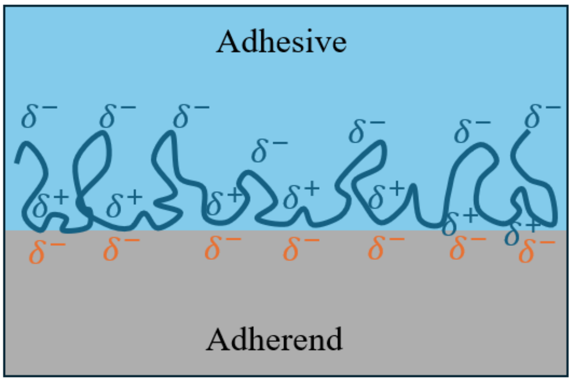

Figure 7: Diagram explaining the electrostatic theory between the adhesive (in blue), which is composed by long molecule chains (in dark blue), and the adherend (in gray). Due to the difference in electronic properties there is a transfer of electrons across the interface, resulting in the creation of regions that are positively (δ^+) and negatively (δ^-) charged.

This mechanism is conceptually similar to the formation of parallel plate capacitor, meaning that there is an storing of electrostatic energy in the interface. The strength of the interaction depends mainly on the electronic properties of the materials. [20]

The electrostatic theory is particularly relevant for systems involving dissimilar materials, such as polymers bonded to metals, where differences in electronic affinity may promote charge separation. However, in practical adhesive systems, the contribution of electrostatic forces is generally considered to be limited and not relevant compared to other mechanisms. In addition, environmental factors such as humidity and the presence of undesired conductive media can dissipate accumulated charges, further reducing the significance of electrostatic effects. Therefore, while the electrostatic theory provides a useful conceptual framework, it is rarely seen as the dominant mechanism responsible of the adhesion. [17]

4.4 Diffusion theory

The diffusion theory of adhesion is based on the idea that bonding occurs through the interpenetration of polymer chains across the interface between two materials. When two compatible polymers are in contact and the molecular mobility is high enough, chains from each polymer can diffuse into the other, forming an interconnected network that favours the adhesion. [20]

This mechanism is highly dependent on factors such as molecular compatibility, temperature and time. Diffusion is more likely to occur when the polymers have similar chemical structures and when the temperature is high enough to allow chain mobility, typically near or above the glass transition temperature (T_g). [17]

Diffusion-caused adhesion is most relevant in polymer–polymer systems. In contrast, for systems involving a polymer adhesive and a metallic substrate, such as the one considered in this work, the potential for molecular interdiffusion is extremely limited due to the absence of chain mobility in the metal. [20] Consequently, the contribution of diffusion to adhesion in adhesively bonded gasket–metal interfaces is expected to be negligible.

4.5 Chemical bonding and interaction forces

Chemical bonding and intermolecular interaction forces are among the most important mechanisms controlling adhesion, particularly in systems involving polymers bonded to metallic substrates. Unlike mechanical interlocking, which depends on surface morphology, these mechanisms originate from interactions at the atomic and molecular scale across the adhesive–adherend interface. [17]

From a chemical point of view, interatomic interactions can be broadly classified into primary and secondary bonds. Primary bonds involve the direct sharing or transfer of electrons between atoms. Primary bonds include covalent bonds, ionic bonds and metallic bonds. These interactions are characterized by high bond energies, typically in the range of 100–1000 kJ/mol, providing a very strong adhesion. However, since sharing of electrons requires direct atomic contact and chemical compatibility between the adhesive and the substrate, primary bonds act only over very short distances, on the order of a few ångströms ($\sim 10^{-10} m$). [18]

On the other hand, secondary interactions are attributed to electrostatic interactions between permanent and/or induced dipoles. These include van der Waals forces and acid-base interactions, which are generally weaker, with bonding energies below 100 kJ/mol. Despite their lower strength these interactions play a crucial role in adhesion because they can act over larger interatomic distances and do not require specific chemical reactions to occur. [18] Van der Waals forces are particularly important, as they are universally present between all atoms and molecules. They originate from fluctuations in electron density that create instantaneous dipoles, which create induced dipoles in neighbouring atoms. The resulting bonding force decreases with distance following an inverse power law dependence often approximated as proportional to r^{-6} for energy and r^{-7} for force. [19]

In the case of acid–base interactions the adhesion is described in terms of Lewis theory, where an electron donor (base) interacts with an electron acceptor (acid). These interactions are particularly relevant at polymer–metal interfaces, where functional groups in the adhesive (such as hydroxyl or ether groups in epoxies) can interact with oxide layers present on metallic surfaces. Hydrogen bonding can be understood as a specific case of acid–base interaction, in which a hydrogen atom that is covalently bonded to an electronegative atom (such as oxygen or nitrogen) acts as an acceptor and interacts with a single pair of another electronegative atom. [17] Overall, although individually weak, secondary interactions can collectively generate significant adhesion when a large contact area is achieved, as is the case of a sample with a good wetting. [18]

In epoxy-based adhesives, both primary and secondary interactions contribute to adhesion. Covalent and acid–base interactions form between reactive groups in the adhesive and hydroxylated oxide layers on metallic surfaces, while van der Waals forces and hydrogen bonding provide an additional contribution across the entire interface. The combined effect of these interactions, distributed over a large area, is responsible for the high adhesion strength typically observed in epoxy–metal systems. [9]

It should be noted that these interactions are highly sensitive to the interfacial distance.

Even nanometer-scale separations caused by poor wetting or contamination can drastically reduce their effectiveness. Therefore, achieving intimate contact between the adhesive and the substrate is crucial for maximizing the contribution of chemical bonding and intermolecular forces.

4.6 Weak boundary layer

The weak boundary layer (WBL) theory does not describe a mechanism of adhesion itself, but rather explains why adhesion may be significantly reduced in some systems. According to this concept, a weak layer present at or near the substrate surface can act as the limiting factor in adhesion performance, regardless of the intrinsic properties of the adhesive. Weak boundary layers may consist of contaminants such as oils, greases or other residues, as well as poorly bonded oxide layers or absorbed humidity. These layers typically have a low internal strength and a poor adhesion to the underlying substrate, causing failure to occur within the boundary layer. [10]

In many cases, what appears to be an adhesive failure is in fact a cohesive failure within a weak interfacial layer, leading to a significant underestimation of the true adhesive potential. [17] In the context of gasket bonding in plate heat exchangers, the formation or evolution of weak boundary layers may be influenced by operational and cleaning conditions. Exposure to humidity, elevated temperatures or chemical cleaning agents can modify the surface chemistry or cause degradation at the interface, which promote the development of weak boundary layers, ultimately reducing the bond strength and serviceability. For this reason, a proper surface preparation accompained by a control of environmental exposure is essential to minimize the formation of weak boundary layers and ensure reliable adhesive performance.

4.7 Unified theory of adhesion

Although several theories have been proposed to explain adhesion, none of them alone is capable to fully describe the behaviour of real adhesive systems. Instead, as mentioned earlier, adhesion is understood as the result of multiple mechanisms acting simultaneously, each contributing in a different scale of action to the overall strength. From this perspective, the total adhesion strength (ϕ) can be conceptually expressed as a weighted combination of the contributions from the different mechanisms:

$$\phi = \alpha\phi_{MI} + \beta\phi_T + \gamma\phi_E + \delta\phi_D + \epsilon\phi_C + \zeta\phi_{WBL} + ... + \omega\phi_X \tag{4}$$

Under the condition of normalization:

$$\sqrt{\alpha^2 + \beta^2 + \gamma^2 + \delta^2 + \epsilon^2 + \zeta^2 + ... + \omega^2} = 1 \tag{5}$$

Where each term represents the contribution of a specific adhesion mechanism: mechanical interlocking (MI), thermodynamic theory (T), electrostatic interactions (E), diffusion (D), chemical bonding and intermolecular forces (C), weak boundary layer effects (WBL), and other theories that are yet to be developed (X). The coefficients $\alpha, \beta, \gamma, \delta, \epsilon, \zeta, ...\omega$ represent the relative weight of each mechanism. [20]

This formulation is not intended to work as a predictive model, but rather as a conceptual model highlighting that adhesion is, by nature, multi-causal. The relative importance of each contribution depends on factors such as material compatibility, surface condition, environmental exposure or loading conditions.

In the specific case of adhesively bonded gasket–metal interfaces, it is expected that thermodynamic effects (wetting), chemical interactions and mechanical interlocking will dominate, while diffusion and electrostatic contributions will remain in a secondary place. The weak boundary layer concept is expected to play a critical role in limiting the effective strength of the interface. Finally, a table is included summarizing the adhesion theories discussed, along with their scale of action:

Theory	**Main mechanism**	**Scale of action**
Mechanical interlocking	Physical anchoring in surface roughness	Microscopic
Thermodynamic theory	Minimization of interfacial energy	Microscopic
Electrostatic theory	Electrical double layer formation	Molecular
Diffusion theory	Interpenetration of polymer chains	Molecular
Chemical bonding and intermolecular forces	Primary and secondary bonds	Atomic / Molecular
Weak boundary layer	Weak interfacial regions	Molecular

Table 1: Summary of the different theories of adhesion and their respective scale of action. [17]

5 Rubbers

Rubbers, also known as elastomers, are widely used in gasket applications due to their ability to undergo large reversible deformations while maintaining sealing performance. Their relatively low elastic Young modulus, high flexibility and good resilience against any type of chemicals, make them particularly suitable for applications involving repeated mechanical loading and thermal cycling, such as gasketed plate heat exchangers. Elastomers are typically composed of crosslinked polymer networks, which allow them to strain significantly and recover their original shape once the pressure on them is released. Their mechanical response differs significantly from the behaviour of metals or rigid polymers, as it is governed by entropic elasticity rather than merely the stretching of the bonds. This entropic elasticity property means that the recovery force comes from the tendency of polymer chains to return to a more disordered and higher-entropy configuration rather than from the stretching of chemical bonds. [21]

Alfa Laval uses many different types of gaskets, but the most common ones, and the ones that have been the center of attention during this thesis, are NBR and EPDM.

- **Nitrile Butadiene Rubber (NBR)** is a copolymer of acrylonitrile and butadiene that is widely used in industrial sealing applications due to its excellent resistance to oils, fuels and many chemical agents. The presence of polar nitrile groups enhances its chemical resistance, specially against non-polar mediums, while also having a great affinity with adhesives (since they are normally polar). [22]

  From a mechanical perspective, NBR exhibits typical elastomeric behaviour, with a relatively low elastic modulus ($E = 6MPa$) and high elongation at break. Its properties can be tuned by adjusting the acrylonitrile content and the degree of crosslinking, allowing optimization for specific applications. [23]

- **Ethylene Propylene Diene Monomer (EPDM)** is a non-polar elastomer known for its excellent resistance to water-based environments, oxidation and ageing. These properties make it particularly suitable for applications involving hot water or steam, which are common in heat exchanger systems. [22]

> Compared to NBR, EPDM generally exhibits lower oil resistance which is compensated by greater thermal stability and less oxidation. The major drawback is that due to its non-polar nature, a poorer adhesion performance is expected, particularly in relation to polar adhesives such as epoxies. In terms of mechanical properties, it is very similar to NBR, with the same elastic modulus ($E = 6MPa$) and high elongation at break, although it breaks slightly easier than NBR. [24]

NBR and EPDM exhibit complementary properties primarily due to their difference in polarity. NBR, defined as a polar elastomer, offers a good resistance to oils and fuels, while EPDM, a non-polar elastomer, provides an excellent performance in water-based and oxidative environments. This complementarity makes these two rubbers suitable for different operating conditions and also makes gasketed plate heat exchangers highly versatile, being able to adapt to all kinds of customer requirements. [25]

When it comes to the application of gaskets in GPHEs, the choice of gasket material is of great importance, but so too is its geometry. The gaskets used typically feature a characteristic "peak" profile, designed to ensure effective sealing when compressed between plates. This geometry allows the gasket to deform under load, creating localized pressure regions that enhance the sealing performance.

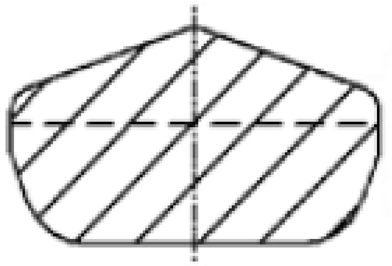

Figure 8: "Peak"-shape gasket profile used. [26]

In terms of tensile behaviour elastomers exhibit a nonlinear stress–strain response. At small deformations, there is an approximately linear behaviour that helps to define an effective Young's modulus. However, as deformation increases, the material behaviour becomes nonlinear. Moreover, unlike metallic materials, elastomers do not exhibit a well-defined plastic region. Instead, their deformation is mainly elastic but time-dependent, with viscoelastic effects such as hysteresis and stress relaxation playing an important role. Upon further loading, failure occurs without a clear elasticity limit being reached. [21]

This mechanical behaviour is particularly relevant in peel testing, where large deformations are induced in the gasket material. The ability of the elastomer to deform and dissipate energy can significantly influence the measured adhesion strength. Therefore, it is necessary to consider both adhesive and elastic energy contributions to the overall response in order to achieve a good estimation of the adhesive performance.

6 Peel testing

The main experimental method used during the project to quantify and evaluate the performance of the different adhesives was peel testing. Peel testing is a widely used experimental technique for evaluating the adhesion performance of bonded systems, particularly when flexible adherends are involved. This characteristic makes peel testing especially suitable for evaluating the adhesion of elastomeric materials (such as gaskets) bonded to rigid substrates (such as plates). This technique measures the force required to debond the gasket from the plate, generating graphs of force as a function of the debonded distance. [27] However, graphs are not easy to interpret since the measured peel force is not only a function of the interfacial adhesion strength, but also depends on the mechanical properties of the adherends, particularly the deformability of the elastomer. In contrast to simple tensile or shear tests, peel tests introduce a highly non-uniform stress distribution, with stresses concentrated at the crack tip where the debonding happens. [28] Therefore, the interpretation of peel test results requires a combined understanding of fracture mechanics, interfacial adhesion and the mechanical response of the materials involved.

6.1 Peel testing theory

As mentioned earlier, peel testing results interpretation is not an easy task, in fact, there is a whole science behind this experimental technique. From a theoretical perspective, peel testing can be interpreted within the framework of fracture mechanics. The debonding process can be defined as the propagation of an interfacial crack and the measured peel force is directly related to the energy required to advance this crack along the interface. [10] Figure 9 shows a diagram and a picture of the experimental setup for the peel test. It consists of a tensile testing machine which uses a hook to grip one end of the flexible adherend, which in this case is the gasket, and begins to pull it upwards at a constant speed, measuring the force exerted as a function of distance, which corresponds to the debonding distance. This process in which the gasket peels away from the metal plate is done at a perpendicular angle, meaning that the method to be studied is a 90-degree peel test. Two cylinders are used to facilitate the 90 degree peeling by rolling the plate while is being peeled.

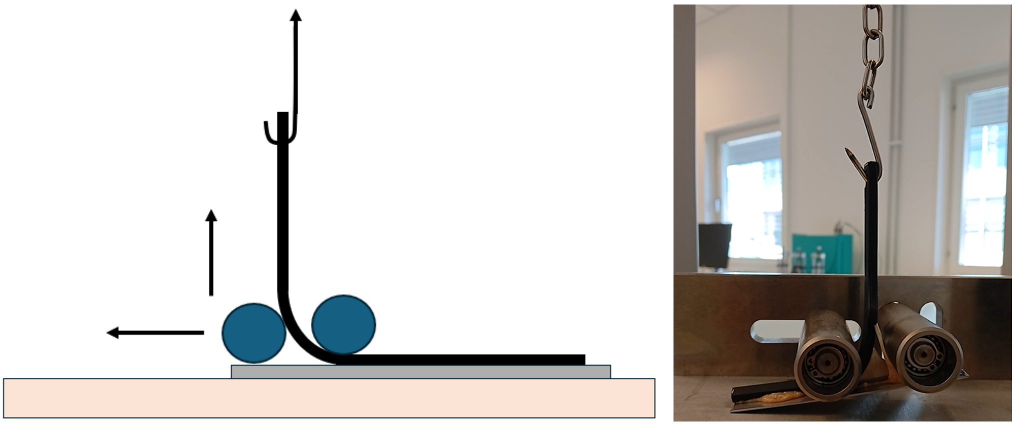

(a) (b)

Figure 9: (a) Diagram representing the peel test experimental set up. A flexible adherend (the gasket, in black) is being pulled upwards with a hook perpendicularly to the plate (in gray) with the help of two cylinders (in blue). (b) Picture of the experimental set up used for peel testing.

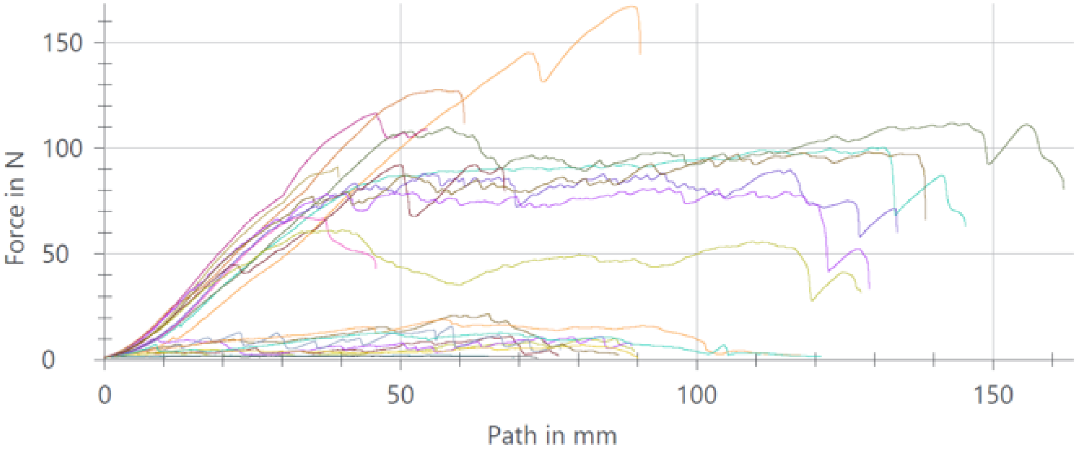

Figure 10: Peel testing curves example.

Figure 10 shows an example of some curves obtained after peel testing. The shape of these curves is clearly determined by the type of adhesive and the failure mode; the latter will be discussed in more detail in Section 6.2. Peeling curves are difficult to interpret and extract a reliable quantifiable parameter from. However, they all share certain similarities. Initially, the hook begins to pull upwards and a linear relationship between force and distance is observed, meaning that the machine is pulling upwards but there is no debonding; rather, the gasket is being elongated. Depending on the strength of the adhesive bond, this linear regime lasts for a longer period (high-performance adhesives) or a shorter period (low-performance adhesives). At a certain point, a maximum force F_{max} is reached and there are two possibilities: either the adhesive bond is so strong that the gasket breaks, and therefore the machine stops measuring as there must be at least 1N of force, or the curve stabilises at a plateau, which is the stable regime. In this regime we find the critical force for peeling F_c, in other words, the exact force required to separate the joint from the metal. Due to irregularities in the interface, the plateau is not completely stable, but it is possible to calculate an average critical force over a debonded distance defined as $a = a_2 - a_1$, where a_1 and a_2 are the initial and the final debonding points:

$$F_c = \frac{1}{a}\int_{a_1}^{a_2} F(x)dx \tag{6}$$

However, the critical force for peeling alone is not sufficient to describe the peeling process in its entirety, neither represents the adhesive's performance accurately, as it does not take into account the elastic contribution of the gasket or the area of the bonded zone. The key parameter for describing this process is the energy release rate G defined as the energy per unit area that is released in the system when the metal is separated from the gasket. This energy is defined by the external work done W, the elastic energy U_E of the peel arm, in this case the gasket, and the area A that is detached in the process. [27]

$$dW - dU_E = G \cdot dA \tag{7}$$

Both elastic energy and work are defined by the external force F exerted, the debonded length a and the elastic deformation ε (the strain) of the gasket: [27]

$$U_E = \frac{1}{2}Fa\varepsilon \qquad ; \qquad W = Fa(1+\varepsilon) \tag{8}$$

Elastic deformation can also be redefined by applying Hooke's law:

$$\varepsilon = \frac{\sigma}{E} = \frac{F}{Ewt} \tag{9}$$

Where w is the width of the bonded area, which in this case is assumed to coincide with the width of the base of the gasket, E is Young's modulus, σ is the strain, and t is the thickness of the gasket. Combining equations (7), (8) and (9) and defining the area as $dA = wda$, the following expression for the energy release rate is obtained:

$$G = \frac{1}{w}(\frac{dW}{da} - \frac{dU_E}{da}) = \frac{F}{w} + \frac{F^2}{2Ew^2t} \tag{10}$$

In order to calculate the critical energy release rate G_c in the steady state regime over a debonding distance a, the following expression is needed:

$$G_c = \frac{1}{a}\int_{a_1}^{a_2} \frac{F(x)}{w} + \frac{F^2(x)}{2Ew^2t}dx \tag{11}$$

Equation (11) is of great importance and will be used in the subsequent analysis of the samples, but it can be further developed. Taking Equation (10) as a starting point, for the particular scenario in which the exact force to separate the interface and to propagate a crack is exerted($F = F_c$), which means that the system releases an energy equivalent to the critical energy release rate ($G = G_c$), it gives the following expression for the critical peeling force:

$$\frac{F_c}{w} = -Et + \sqrt{E^2t^2 + 2EtG_c} = -Et + Et\sqrt{1 + \frac{2G_c}{Et}} \tag{12}$$

Since $E \sim 6$ MPa, $t = 5.70mm$ and G_c varies from $G_c \sim 100 - 300N/m$ for the weakest adhesives to $G_c \sim 2000 - 5000N/m$ for the strongest adhesives, it is possible to assume $\frac{2G_c}{Et} << 1$ only for weak adhesives. Applying Taylor's approximation: for $x << 1$, $\sqrt{1+x} \simeq 1 + \frac{x}{2}$; it is finally obtained the following expression that relates the critical force and the critical energy release rate:

$$\frac{F_c}{w} = G_c \tag{13}$$

This expression shows that although the elastic term was initially considered in Equation (7), it does not contribute to the calculation of the critical energy release rate when weak adhesives are used. Combining Equation (6) and Equation (13) it is finally obtained another expression that computes the critical energy release rate:

$$G_c = \frac{1}{wa}\int_{a_1}^{a_2} F(x)dx \tag{14}$$

6.2 Failure modes

Failure mode has a significant impact on the peel test results, indeed, it is essential to include a section only for explaining in detail the physics behind each failure mode and what it implies. It is possible to draw an analogy in which the adhesion of two surfaces can be seen as a bridge connecting two banks. In this model, there are two types of forces. First, there is the adhesive force, which is responsible for the bond between the adhesive and the adherend. In our analogy, this force represents the foundations of the bridge. Secondly, there is the cohesive force, in other words, the internal force of the adhesive and the adherend themselves, which in the analogy corresponds to the strength of the bridge itself and the margins upon the bridge is anchored (adherend). As with the bridge, when the adherend-adhesive-adherend system is exposed to extreme external conditions, such as peel testing, at some point the adhesive bond fails. [18]

"An adhesion bond will fracture at its weakest link", [10] this statement from Souheng Wu, as simple and trivial as it might seem, is the explanation of the variation in failure modes. There are five possible failure modes for the gasket to metal bond that are represented in a diagram in Figure 11 for a better understanding. [16]

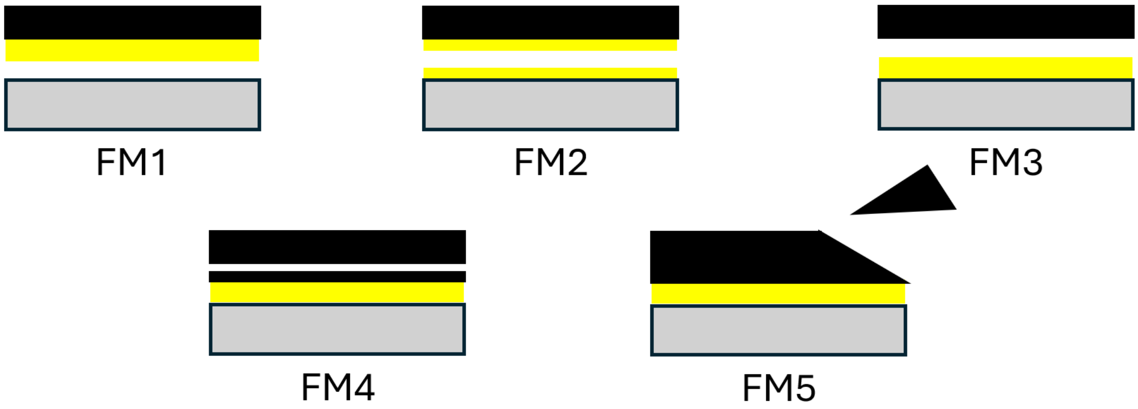

Figure 11: Diagrams representing all five possible failure modes after peel testing in a system composed of a metal (in gray) that is adhesively bonded to a gasket (in black) through and adhesive (in yellow).

- **Failure mode 1 (FM1)**: Adhesive failure to the metal plate. The adhesive peels away from the metal because adhesion at that boundary is the weak point of the system.
- **Failure mode 2 (FM2)**: Cohesive failure of the adhesive. The failure occurs within the adhesive itself. The adhesion to the adherends is stronger than the internal strength of the polymer, and the adhesive breaks internally.
- **Failure mode 3 (FM3)**: Adhesive failure to the gasket. The adhesive peels away from the gasket because adhesion at that boundary is the weak point of the system. In this case the adhesive force to the gasket is weaker than that to the metal or the cohesive force of the adhesive itself.
- **Failure mode 4 (FM4)**: Cohesively delamination of the gasket. The gasket internally fails but remains the part that is bonded to the adhesive.
- **Failure mode 5 (FM5)**: Cohesive failure of the gasket. The adhesive bond is so strong that the failure occurs in one of the adherends (in this case the gasket), away from the bond.

In terms of adhesive performance the desired situations are FM4 and FM5, which means that the adhesive is strong enough that the weakest point of the system is not the adhesive but the gasket itself. When a FM4 or FM5 is achieved it means that the operational limit of a GPHE is constituted by the integrity of the gasket.

It should be noted that despite failure modes FM1, FM2 and FM3 might be grouped as an "adhesive failure", it is of great importance to differentiate them in order to determine where is the weak point of the system: the interface adhesive-metal, the interface gasket-adhesive or the internal strength if the adhesive itself.

As commented above, failure modes are mainly responsible for the peel curves shape, in fact, just by looking at the curves it is possible to deduce which failure mode is involved. Using Figure 10 as a reference, a failure mode can be assigned to each curve depending on the range of forces reached and the debonding length. If maximum forces exceeding 40–50 N are reached, FM1–3 are no longer observed and the adhesive is considered strong. [29] Among strong adhesives, two scenarios can occur: the gasket breaks (FM5), implying a very short debonding length, or the gasket delaminates cohesively (FM4), resulting in a very long debonding length.

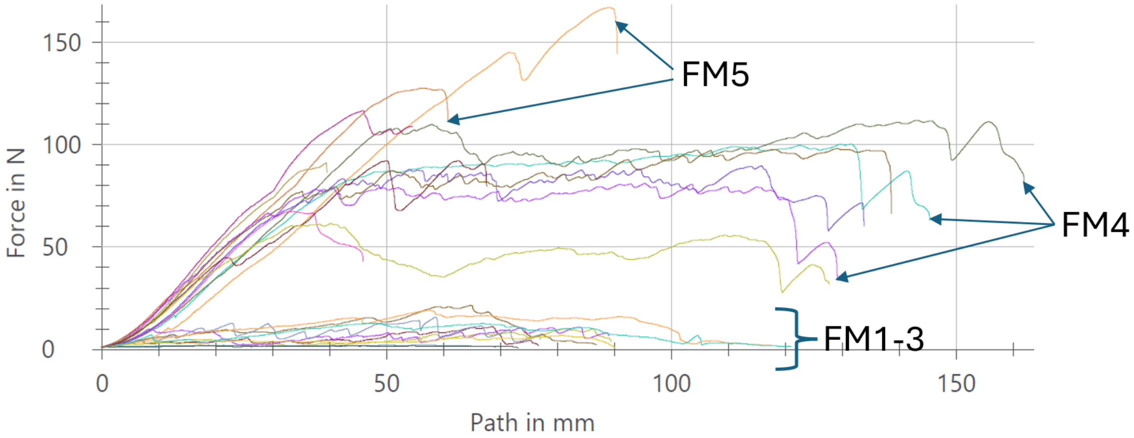

Figure 12: Peel testing curves and their corresponding failure mode.

7 Water jetting

While peel testing provides a controlled method to evaluate adhesion performance, it does not fully represent the conditions experienced by gasketed plate heat exchangers during service. In practice, these systems are periodically cleaned to remove fouling deposits using high-pressure water jetting techniques. [8] Therefore, the objective of this work is not only to examine the adhesive performance under ideal conditions, but to evaluate the serviceability of adhesively bonded gaskets under realistic cleaning conditions, where mechanical and hydraulic loads are imposed on the adhesive joint. Among the various cleaning methods, water jetting is widely used due to its effectiveness in removing deposits without the need of chemical agents despite the potential risk to the adhesives joints. [30]

Water jetting is a cleaning technique based on the projection of a high-pressure water jet onto a surface. The cleaning effect is primarily achieved through the transfer of momentum from the water jet to the contaminants and the substrate surface, generating impact forces that remove deposits. The intensity of this interaction depends on several process parameters, which control both the energy delivered to the surface and its spatial distribution. The most relevant parameters governing water jet cleaning are [31] [32]:

- **Water pressure:** is one the most influential parameter, as it directly determines the jet velocity and, consequently, the impact force exerted on the surface. Higher pressures result in increased kinetic energy and more effective removal of deposits, but also lead to higher stresses at the interface, potentially damaging or debonding the adhesive layer.

- **Flow rate:** complements the effect of pressure by controlling the total volume of water transferred per unit of time. While pressure defines the intensity of the jet, the flow rate determines the total energy input, influencing the extent and uniformity of cleaning.

- **Nozzle-surface distance:** controls energy dissipation before impact. As the jet travels through the air there is dispersion and energy dissipation. Therefore, shorter distances result in a more concentrated and aggressive jet, while larger distances reduce impact intensity and increase the affected area.
- **Spraying angle:** determines the relative contribution of normal and shear stresses acting on the joint. At normal incidence (90°), the jet primarily generates impact and compressive forces, whereas at lower angles shear forces become more significant. These shear components are particularly effective for the removal of adhered contaminants but it also has a greater impact on the adhesive bond, promoting crack propagation along the interface.
- **Water temperature:** can influence the behaviour of the adhesive. Elevated temperatures enhance cleaning efficiency, but it also affects the mechanical properties of the adhesive, particularly if the temperature approaches the glass transition temperature (T_g).
- **Exposure time:** represents the cumulative effect of the cleaning loading. Even though at first it may look that it does not cause immediate damage, repeated exposure may lead to progressive degradation of the adhesive joint through mechanisms such as erosion or moisture penetration.
- **Sweeping speed:** defined as the velocity at which the jet is moved across the surface, it controls the exposure time per unit of area. Lower sweeping speeds result in longer exposure and higher cumulative energy input, increasing both cleaning effectiveness and the risk of damage. On the contrary, higher speeds reduce exposure time and result in gentler cleaning conditions.

In addition to these process parameters, the design of the nozzle plays a crucial role in defining the characteristics of the water jet. The nozzle geometry determines the spatial distribution of velocity, pressure and transferred, hence influencing both cleaning performance and the level of mechanical loading applied to the surface. The following types of nozzles are available [32]:

- **Straight jet or orifice nozzles:** produce a highly concentrated jet with minimal dispersion, resulting in a very high local energy density. These characteristics makes them particularly effective for localized removal of strongly adhered deposits but it also risks mechanical damage or adhesive failure.
- **Rotary nozzles:** introduce a rotational motion to the jet. This rotation distributes the jet over a larger surface area, reducing the local energy density while maintaining a relatively high cleaning efficiency. As a result, rotary nozzles are commonly used for cleaning large surfaces, such as heat exchanger plates, where a uniform treatment that combines power and cleaning speed is required.
- **Fan jet nozzles:** also known as flat spray nozzles, they generate a wide and thin jet with a uniform distribution of water across its width. This results in a more homogeneous and less aggressive cleaning action. They are suitable for removing loosely adhered contaminants without causing deep erosion.

- **Multi-jet heads:** divide the flow into several smaller jets, distributing the energy more evenly across the surface. This reduces greatly the intensity of individual impacts and leads to a gentler cleaning process.

For a better understanding, it is shown a diagram with three of the most popular nozzle types and their respective spray patterns:

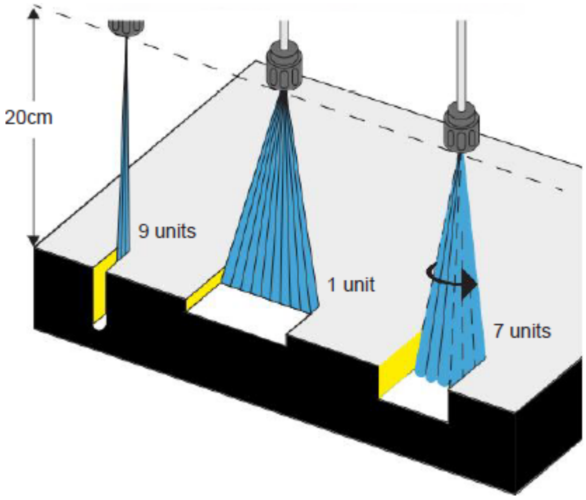

Figure 13: Diagram representing the spray pattern and depth force for an orifice nozzle (on the left), a fan jet nozzle (in the middle) and a rotary nozzle (on the right). “Units” in this case are used as an arbitrary measure of length for the purpose of showing a comparative analysis of the range of each jet. [30][32]

Overall, the choice of nozzle type involves a trade-off between cleaning efficiency and the risk of damage, and must be carefully considered when evaluating the serviceability of adhesively bonded systems under water jetting conditions.

8 Factors that affect the adhesion

The adhesion performance of bonded gasket systems is determined by a combination of material properties and compatibility, interfacial phenomena and external loading conditions. As discussed in the previous sections, adhesion is not controlled by a single mechanism, but rather emerges from the interaction of multiple factors acting across different length scales at the same time. In the context of this study, it is essential to identify and summarize the most relevant parameters that influence adhesion in a gasket-plate system. It should be noted that this section is intended to provide a solid framework for the correct interpretation and a deep understanding of the experimental results.

The first thing to highlight are the intrinsic properties of both the adhesive and the adherends (in this case the gasket and the plate), which play a fundamental role in determining adhesion performance. For epoxy-based adhesives, key parameters include crosslink density and glass transition temperature (Tg), which control stiffness, thermal stability and resistance to environmental degradation. These properties directly influence the ability of the adhesive to sustain mechanical loads, chemical exposure and resist softening under cleaning conditions. On the other hand, the nature of the rubber substrate is also critical. NBR and EPDM exhibit distinct chemical and mechanical behaviours caused mainly by their different polarity and network structure. While NBR may provide a better compatibility with adhesives (since all adhesives used are polar), EPDM offers a superior resistance to water and thermal ageing. Another fact to consider is their elastomeric nature, which introduces significant deformation and energy dissipation during loading, particularly in peel conditions.

In addition to the intrinsic properties of the adherends, it is crucial to consider interfacial phenomena to explain adhesion performance. Adhesion is strongly influenced by the conditions at the adhesive–substrate interface. Proper wetting and surface energy compatibility not only enables intimate molecular contact and promotes a high work of adhesion (as shown in Equation (2)), but it also allows intermolecular interactions and chemical bonding to develop. The combined contribution of chemical bonding, van der Waals interactions and acid–base interactions depends largely in intimate molecular contact and it ultimately determines the intrinsic strength of the interface.

Other interfacial effects are surface roughness and contamination. The first one enhances adhesion through mechanical interlocking, in fact, it has been proven in previous studies at Alfa Laval that gaskets with a higher porosity or with a pretreatment that maximizes roughness perform better. [29] The latter is related with the presence of weak boundary layers and can severely reduce effective adhesion by introducing mechanically weak regions at the interface.

In order to evaluate the performance of adhesives peel testing is used, a method that is not only a function of interfacial properties, but it also depends on the mechanical response of the bonded system. After a deep analysis of the physics behind this experimental method, two models have been developed that relate the exact force (F_c) and energy (G_c) required to propagate a crack in the interface and to separate the gasket from the metal. On the one hand, there is a complex model defined by Equation (11), which demonstrates that the deformation of the elastomer plays a major role. This means that in order to separate the gasket from the metal, an energy equal to the fracture energy is not sufficient, but the contribution of elastic energy must also be considered. On the other hand, there is a much simpler model defined by Equation (14), which is only valid for weak adhesives, that weak that the energy used to separate the adhesive system is equivalent to the fracture energy. The elastic contribution is negligible when such small forces are applied.

Environmental factors such as temperature, moisture and chemical exposure can significantly affect the adhesion performance. These factors may alter the mechanical properties of the adhesive, reduce its glass transition temperature or promote chemical degradation at the interface. In particular, exposure to water and elevated temperatures during cleaning processes may accelerate degradation mechanisms, leading to a reduction in adhesion strength over time. The cleaning process itself introduces additional mechanical loading on the adhesive joint. Parameters such as water pressure, nozzle-surface distance, spraying angle or exposure time determine the magnitude and distribution of stresses applied to the interface. These loads may induce crack initiation or propagation, especially in regions where adhesion is already weakened by environmental effects or interfacial defects. Therefore, the interaction between cleaning parameters and material properties is a key aspect in evaluating gasket serviceability.

9 Experimental results and Discussion

9.1 Samples

In order to analyze the behaviour of gaskets in GPHEs, it is necessary to scale the analysis to a smaller, more manageable and yet reproducible system. Figure 14 shows a diagram with the measurements of the samples created during the thesis. It consists of a 100.0 mm long stainless steel plate bonded to a 140.0 mm long gasket (either NBR or EPDM). This extra length is essential and very helpful for subsequent peel testing.

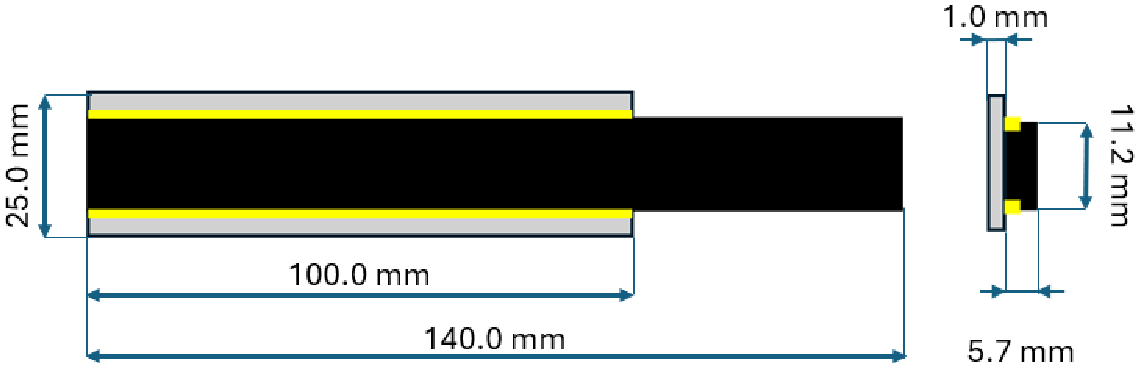

Figure 14: Diagram representing the samples created in order to study adhesively bonded GPHEs. They are composed by a plate (in gray) which is bonded to a gasket (in black) using an adhesive (in yellow).

The sample manufacturing process is as follows: first, several stainless steel plates and gaskets with the dimensions shown in Figure 14 are collected. In order to ensure a clean surface and avoid weak boundary layers, both surfaces of the samples are cleaned with isopropanol. Once cleaned, they are placed in fume hoods and the adhesive (which is generally kept in freezers to prevent anticipated curing) to be studied is dispensed onto the plate surface. Next, the gasket is placed on the metal plate and pressure is applied. It is crucial to consider two factors to ensure reproducible behaviour that resembles the plate-adhesive-gasket system found in GPHEs. First, the adhesive must be distributed homogeneously over the entire base of the gasket and the same amount of adhesive must be present in all samples. Second, the pressure applied must be the same for all samples and is applied using the fixture shown in Figure 15. Once the glue is applied, all samples are stacked in the fixture, where spacers are placed at the edges to ensure proper compression. The fixture is then tightened with bolts. This process is crucial because the samples are manufactured under the same pressure as the heat exchangers in the factory, in addition it promotes effective wetting.

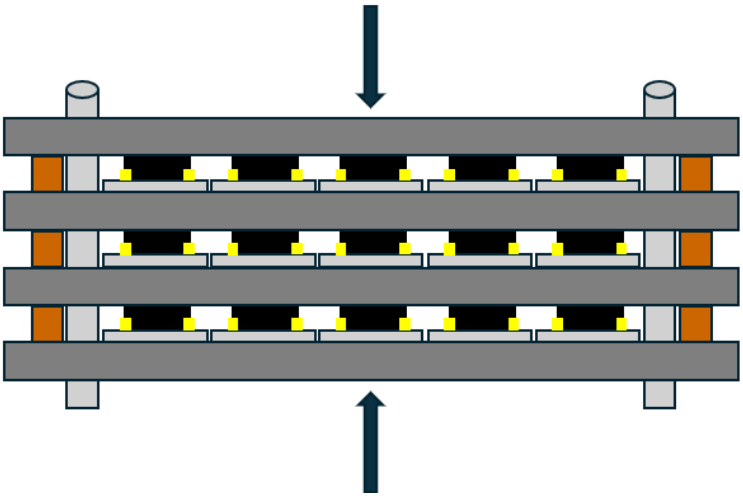

Figure 15: Diagram of the fixture created for ensuring the right compression of the samples during the curing. The right amount of compression is given by the spacers (in orange) which vary depending on the gasket used.

Once stacked and compressed, depending on the adhesive type, the samples are cured at room temperature or in an oven to increase crosslink density. A table listing the four adhesives to be studied and their respective curing methods, as indicated by Alfa Laval, is included below. After the curing time has passed and the desired crosslink density has been reached, the samples are removed from the fixture.

Glue	**Recommended curing method**
GC5	Curing at room temperature.
GC6	Oven cured.
GC8	Curing at room temperature.
GC11	Curing at room temperature.

Table 2: The four adhesives studied and their respective curing methods.

As mentioned in Sections 3.2 and 5, this study focused on two types of gaskets (NBR and EPDM) and four types of adhesives (GC5, GC6, GC8, and GC11). At first glance, it may seem that there are only eight possibilities, but this changes when factors such as crosslink density, ageing and supplier are included. Table 3 shows the set of samples created during the study.

It is worth noting that the GC8A and GC8B adhesives are identical in terms of characteristics (an acrylic nitrile/phenol resin that cures by crosslinking as the solvent evaporates) but are manufactured by different suppliers. This results in slight variations, such as the solvent content, which can lead to small differences in performance.

The curing method is just as crucial as the chemical composition, as it ultimately determines the crosslink density. Crosslink density is a key parameter for assessing adhesive performance. Therefore, both the chemical composition and the curing method of an adhesive are equally important, since the curing process directly influences the final crosslink density. Systems 11, 14 and 15 use a GC6 adhesive cured at temperatures below the recommended range, resulting in a lower crosslink density. These are very interesting samples because they replicate the behaviour of heat exchangers whose manufacturing process was not ideal. System 12, on the other hand, is cured at a temperature higher than the recommended range, which implies a higher crosslink density. In all cases, a difference in performance is expected.

Finally, there is System 13, which consists of a cured GC6 sample with an EPDM gasket, cured under ideal conditions and subsequently subjected to an ageing process in the humidity chamber. This is a very interesting experiment as it emulates the behaviour of heat exchangers after being used for a period of time (although in the humidity chamber the sample is subjected to much harsher conditions).

# System	**Gasket**	**Glue**	**Curing method**
System 1	NBR	GC5	Cured at room temperature.
System 2	EPDM	GC5	Cured at room temperature.
System 3	NBR	GC6	Oven cured.
System 4	EPDM	GC6	Oven cured.
System 5	NBR	GC8A	Cured at room temperature.
System 6	EPDM	GC8A	Cured at room temperature.
System 7	NBR	GC8B	Cured at room temperature.
System 8	EPDM	GC8B	Cured at room temperature.
System 9	NBR	GC11	Cured at room temperature.
System 10	EPDM	GC11	Cured at room temperature.
System 11	EPDM	GC6	Cured in the oven using a temperature $60°C$ bellow recommendations.
System 12	EPDM	GC8A	Oven cured.
System 13	EPDM	GC6	Oven cured + ageing process consisting on 11 days in the humidity chamber at $85°C$ and 95% of relative humidity.
System 14	NBR	GC6	Cured in the oven using a temperature $90°C$ bellow recommendations.
System 15	EPDM	GC6	Cured in the oven, using a temperature $90°C$ bellow recommendations.

Table 3: Summary of the all the systems gasket-glue created and their respective curing method.

Once cured, the samples are ready to be used for peel testing and water jetting.

9.2 Peel testing

Peel testing was carried out in order to evaluate the adhesion performance of the 15 different bonded gasket systems. The peel tests were performed using a Zwick Roell tensile machine using a constant test speed of $100mm/min$ while maintaining a peel angle of approximately 90°. The experiments were carried out at room temperature. This machine is also equipped with a software that records the applied force and displacement during the test, resulting in the force–displacement curves characteristic of the peeling behaviour that have been explained in Section 6. In addition, the software shows the maximum and the average force (F_{max} and F_{av} respectively) exerted during the test. Both parameters have been used in Alfa Laval as a reference for evaluating the system's performance but it should be noted that none of them coincide with the critical peeling force (F_c) defined in Equation (6). The difference between the average force computed by the software and the critical peeling force lies in the interval chosen. The first one is the average force over the entire measured interval, including the linear region in which the gasket is being elongated but there is no debonding, the plateau region where the peel force oscillates around an approximately constant mean value since the gasket is being peeled and there is a crack propagation, and the final region in which a sudden drop in force is observed, meaning that either the debonding of the gasket is completed or the rubber substrate has failed mechanically. In contrast, the critical force is the average force only on the peeling interval, which coincides with the plateau regime.

The determination of the peeling interval defined by a_2 and a_1 in Equation (6) for the computation of the critical force is not straightforward, as peel curves exhibit significant variability depending on the adhesive system and failure mode. Consequently, the selection of the interval inevitably involves a certain degree of interpretation based on the characteristic features of each curve. For strong adhesive systems, the peeling interval is selected within the plateau region, which corresponds to stable crack propagation conditions and therefore provides the most representative measure of the peeling response. An example is shown in Figure 16a.

In contrast, weaker adhesive systems often do not exhibit a well-defined plateau region. In these cases, the peeling interval is decided by analyzing the changes in slope. Initially, the force increases approximately linearly, with the slope being mainly governed by the elastic deformation of the gasket material. However, a transition point is eventually observed where the slope becomes less steep, indicating the initialization of the crack propagation. This transition reflects a change in the energy balance of the system: the energy that is externally supplied is no longer used exclusively for the elastic elongation of the gasket, but is also consumed in propagating the interfacial crack, which ultimately defines the adhesive response. From this point onwards, the system is considered to have entered the peeling regime. Within the peeling region, it is commonly observed force fluctuations due to the formation and rupture of adhesive strings attached to the gasket edges during crack propagation. Nevertheless, the end of the peeling regime is identified by a pronounced drop in force, corresponding to complete debonding of the bonded system. An example of this behaviour for a weak adhesive system is shown in Figure 16b.

Although the exact boundaries of the peeling interval may vary between samples, the same selection criteria were applied consistently throughout the analysis in order to ensure a meaningful comparison between experimental conditions.

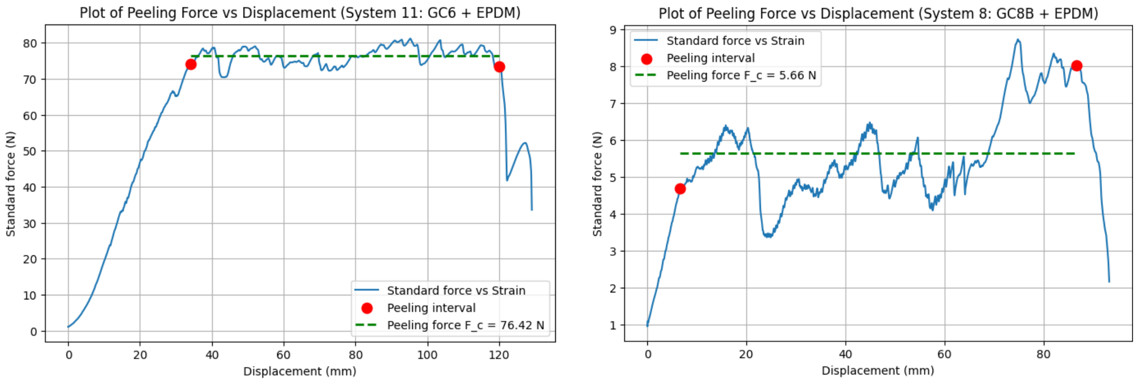

(a)

(b)

Figure 16: Peel testing graph representing the peeling force as a function of the displacement, the peeling interval and its peeling force (F_c) for an (a) strong adhesive (System 11: GC6 + EPDM cured in the oven $60^{\circ}C$ bellow recommendations) with failure mode FM4 and (b) weak adhesive (System 8: GC8B + EPDM cured at room temperature) with failure mode FM3.

It should be noted that for a peel testing that results in a failure mode FM5 no stable peeling interval is observed. In this case, the measured force does not correspond to the force required to propagate an interfacial crack, but rather to the mechanical load sustained by the gasket before rupture occurs. Consequently, a different treatment of the peel curve is required. For FM5 scenarios, the selected interval corresponds to the final portion of the curve immediately before failure, where the maximum force is reached. The calculated value of F_c should therefore be interpreted as a lower limit for the actual critical adhesive force. In other words, at least this force is required to initiate adhesive debonding, but since gasket rupture occurs prior to interfacial failure, the true adhesion limit cannot be determined directly from the test. An example of a peel testing curve corresponding to failure mode FM5 is shown below.

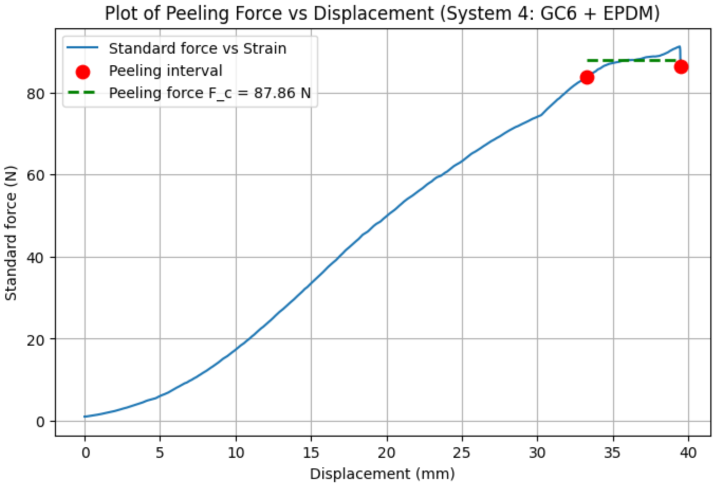

Figure 17: Peel testing graph representing the peeling force as a function of the displacement, the peeling interval and its peeling force (F_c) for a sample composed of GC6 + EPDM cured in the oven (System 4) that resulted in a failure mode FM5.

Therefore, multiple peel tests are carried out for each system, determining for each one the failure mode (FM), the peeling force (F_c), the critical energy release rate using the simple model (G_c) shown in Equation (14) and taking into account the elastic contribution ($G_{c,elastic}$) as shown in Equation (11), and the two parameters provided by the Zwick Roell software that have been used so far at Alfa Laval in order to evaluate the performance of the systems: the average force (F_{av}) and the maximum force (F_{max}).

Due to the inherent variability associated with adhesive joints and elastomeric materials, the experimental error is quantified using 95% confidence intervals based on the Student's t-distribution:

$$CI = t_{0.975,n-1}\frac{s}{\sqrt{n}} \tag{15}$$

Where s is the standard deviation, CI is the confidence interval (the error), $t_{0.975,n-1}$ is the Student's t-coefficient with 97.5% of confidence (leaving a 2.5% of uncertainty on each side) and n is the number of tested samples.

# System	FM	F_{max} (N)	F_{av} (N)	F_c (N)	G_c (kJ/m^2)	$G_{c,elastic}$ (kJ/m^2)
System 1	1	3.5 ± 5.8	2.4 ± 3.1	2.4 ± 3.2	0.27 ± 0.36	0.28 ± 0.37
System 2	1	2.77 ± 0.8	2.12 ± 0.64	2.14 ± 0.65	0.244 ± 0.074	0.245 ± 0.098
System 3	4-5	120 ± 28	72.6 ± 8.9	104 ± 25	11.8 ± 2.8	14.0 ± 3.9
System 4	4-5	91.8 ± 9.8	57.0 ± 7.6	79 ± 14	8.9 ± 1.5	10.2 ± 1.9
System 5	2-3	35 ± 12	19.5 ± 7.1	21.3 ± 7.8	2.42 ± 0.88	2.55 ± 0.96
System 6	3	34 ± 18	17.2 ± 8.9	20 ± 11	2.2 ± 1.2	2.4 ± 1.3
System 7	1	46 ± 15	27.7 ± 9.5	30 ± 10	3.4 ± 1.2	3.6 ± 1.3
System 8	3	14 ± 12	8.0 ± 6.4	8.4 ± 6.9	0.96 ± 0.78	0.99 ± 0.82
System 9	4-5	127 ± 20	77 ± 11	109 ± 21	12.4 ± 2.3	14.8 ± 3.2
System 10	4-5	80.2 ± 6.1	54 ± 10	72.6 ± 6.3	8.26 ± 0.72	9.28 ± 0.89
System 11	4-5	92.0 ± 8.9	66.9 ± 5.1	83.9 ± 8.3	9.69 ± 0.91	10.8 ± 1.3
System 12	4-5	60 ± 16	38.5 ± 8.8	45 ± 13	5.1 ± 1.5	5.5 ± 1.8
System 13	5	91 ± 11	55 ± 13	84 ± 12	9.6 ± 1.4	11.0 ± 1.8
System 14	3	17 ± 12	9.5 ± 3.5	10.9 ± 5.0	1.24 ± 0.57	1.27 ± 0.60
System 15	4-5	60 ± 21	40 ± 13	48 ± 17	5.5 ± 1.9	6.0 ± 2.2

Table 4: Peel testing results showing the failure mode(FM), the parameters given by the Zwick Roell software (F_{max} and F_{av}) and the computed parameters: peeling force (F_c), the critical energy release rate using the simple model (Gc) and taking into account the elastic contribution ($G_{c,elastic}$).

At first glance, it can be observed that some systems exhibit a relatively large experimental dispersion and consequently high uncertainty, resulting in significant relative errors. This variability is characteristic of polymer-based bonded systems, whose mechanical and interfacial behaviour is inherently complex and sensitive to local variations in material properties, surface conditions and crack propagation mechanisms. As a result, adhesive systems often display considerable sample-to-sample variability, making their experimental characterization particularly challenging.

Nevertheless, despite this dispersion, several meaningful trends can still be identified, allowing comparisons between systems and the establishment of a relative ranking based on their bond strength performance. In order to facilitate a clearer visual comparison between the different gasket–adhesive systems, a bar chart showing the representative critical force (F_c) for each system is presented below.

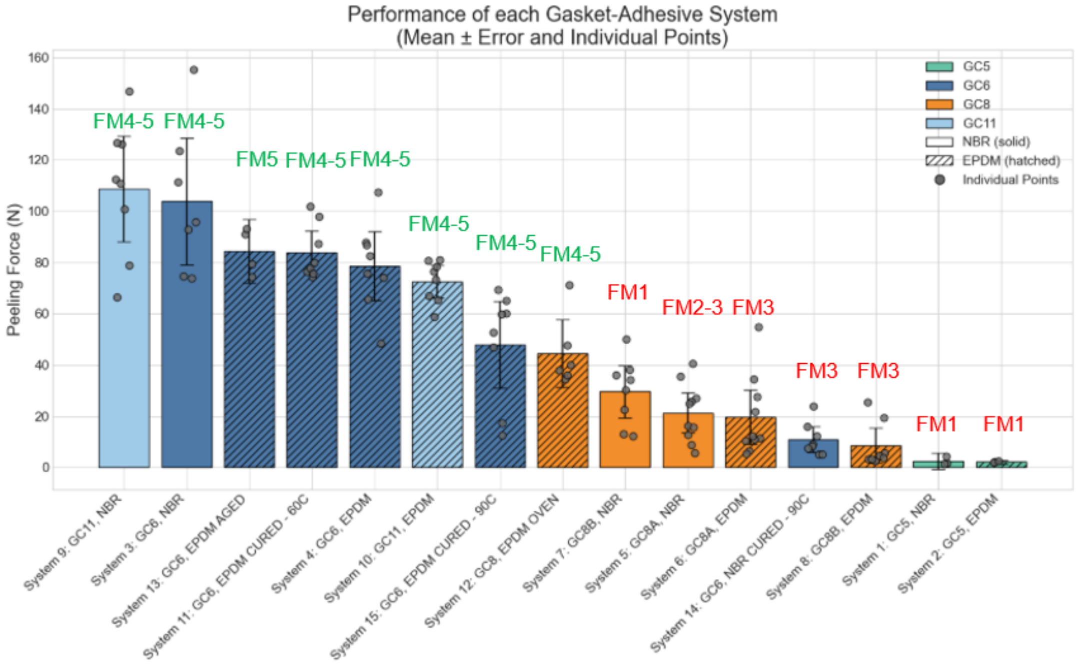

Figure 18: Peeling force (F_c) of each gasket-adhesive system and their respective failure mode, mean, error and individual points. The systems are ordered in a descending way based on their average peeling force.

Firstly, it is immediately evident that Systems 1 and 2, both based on the GC5 adhesive, exhibit the lowest adhesion performance among all the tested configurations. The predominance of failure mode FM1 indicates very poor adhesion to the metallic substrate, suggesting that GC5 provides insufficient interfacial bonding strength for the present application. Therefore, despite being FDA approved, this adhesive appears unsuitable for adhesively bonded gasket systems where high mechanical reliability is required.

In contrast, the nitrile-based adhesive GC8 exhibits a moderate peel strength that is nevertheless significantly higher than that of GC5. Both suppliers, GC8A and GC8B, provide adhesives with relatively similar performance, although GC8A generally appears to achieve slightly higher critical forces. One important advantage of GC8 is that it already provides a certain level of adhesion without requiring oven curing, making it attractive from a processing and manufacturing perspective. However, when oven curing is applied, the representative peeling force increases dramatically, approximately doubling in the case of System 12 compared to System 6. This behaviour strongly suggests the formation of a higher crosslink density during curing, resulting in a stiffer and more mechanically resistant adhesive network. Consequently, a larger amount of energy is required to propagate the crack along the interface during peel testing.

As expected for a nitrile-based adhesive, GC8 also exhibits a noticeably better performance when bonded to NBR gaskets than to EPDM. This observation highlights the importance of chemical compatibility between adhesive and gasket material. Similar polarity and chemical structure can facilitate adhesion mechanisms such as diffusion at the interface and intermolecular interactions associated with chemical bonding theories. Additional evidence supporting this compatibility is provided by the observed failure modes. When EPDM gaskets are employed, failure mode FM3 is predominantly observed, indicating that the adhesive adheres more strongly to the metallic substrate than to the gasket material itself. In contrast, when NBR gaskets are used, a combination of failure modes

FM1–FM3 is observed depending on the supplier. This suggests that, in many cases, the adhesive bond to the gasket becomes comparable to or even stronger than the bond to the metal substrate, and in some cases the limiting factor is the cohesive strength of the adhesive itself (FM2).

Despite these advantages, the major drawback of GC8 is its large experimental variability. The systems based on this adhesive exhibit relatively high standard deviations and large relative uncertainties, indicating considerable sample-to-sample variability. This suggests that the adhesive behaviour is less predictable and potentially less reliable under practical operating conditions.

In contrast to GC5 and GC8, the epoxy-based adhesives GC6 and GC11 exhibit remarkably high bond strength and clearly outperform the other systems investigated in this work. In particular, GC6 represents the reference adhesive employed by Alfa Laval due to its well-known high adhesion performance and mechanical reliability. When cured under the recommended conditions (Systems 3 and 4), extremely high peeling forces are obtained together with the desired failure modes, namely FM4 and FM5. In these cases, the weakest component of the system is no longer the adhesive interface, but the gasket material itself, meaning that the cohesive strength of the elastomer ultimately determines the maximum load the system can withstand.

When GC6 is cured under non-ideal conditions (Systems 11, 14, and 15), a reduction in performance can be observed. Interestingly, curing the adhesive at a temperature $60°C$ below recommendations does not significantly affect the measured performance, indicating that a comparable crosslink density is still achieved under these conditions. However, when the curing temperature is reduced by $90°C$, there is a noticeable decrease in peel strength, particularly in the case of NBR (System 14). This highlights the critical importance of an adequate curing process in order to achieve the desired degree of crosslinking and the corresponding mechanical properties of the adhesive network. The large difference in peeling force between NBR and EPDM under these low-curing conditions can be further understood by analyzing the corresponding failure modes. Under identical curing conditions associated with a lower crosslink density (Systems 14 and 15), the adhesive appears to penetrate and interact more effectively with the EPDM gasket surface than with the NBR gasket, leading predominantly to FM4–FM5 instead of FM3. This suggests that, in the case of NBR, there is an insufficiency of wetting or a reduction of mechanical interlocking at the adhesive–gasket interface, causing this interface to become the weakest region of the system.

Regarding the aged sample (System 13), the measured peeling force remains essentially identical to that obtained for ideally cured GC6 + EPDM systems and for systems cured at temperatures $60°C$ below recommendations (Systems 4 and 11 respectively). This indicates that the ageing process does not significantly affect either the effective crosslink density or the adhesion at the adhesive–gasket interface, and therefore does not alter noticeably the overall performance of the bonded system. This behaviour can largely be attributed to the non-polar nature of EPDM, which results in very limited affinity for water molecules and consequently reduced moisture diffusion through the interface.

Previous studies conducted at Alfa Laval have shown the opposite behaviour when NBR gaskets are employed. Due to the polar nature of NBR, water diffusion through the adhesive–gasket interface is promoted, potentially reducing wetting quality, weakening intermolecular interactions and chemical bonding at the interface. Under ageing conditions comparable to those investigated for System 13, NBR-based samples similar to System 12 may eventually experience complete gasket detachment from the metallic substrate. Nevertheless, it should be emphasized that ageing processes remain inherently statistical in nature. Although EPDM itself is non-polar, GC6 is an epoxy-based adhesive and therefore possesses polar character. Consequently, there is a chance that localized reductions in peeling force may occur in certain samples due to moisture-related effects in the interface. While such degradation was not observed in the tested samples, the possibility cannot be completely excluded, further highlighting the stochastic nature of adhesion degradation phenomena.

Finally, the two-component epoxy adhesive GC11 demonstrates exceptionally high performance, comparable to that of GC6, while eliminating the need for oven curing. This remarkable adhesion performance is primarily attributed to the very high crosslink density achieved even at room temperature curing conditions, resulting in a mechanically robust and highly resistant adhesive network. As it was the case with GC6, the limiting factor of the system is the cohesive strength of the gasket (failure modes FM4 and FM5).

Another important point concerns the apparent performance difference between the two gasket materials investigated, namely NBR and EPDM, which possess significantly different chemical and mechanical characteristics. With the exception of GC6 cured at a temperature $90°C$ below recommendations, the NBR-based systems generally exhibit higher measured peeling forces than their EPDM counterparts. However, the origin of this behaviour depends strongly on the adhesive system considered. In the case of the nitrile-based adhesive GC8, the improved performance observed with NBR can be primarily attributed to the greater chemical affinity between the adhesive and the gasket material. Since both the adhesive and the NBR gasket possess nitrile components, stronger intermolecular interactions can develop at the interface, potentially promoting adhesion mechanisms such as diffusion and chemical bonding. As a result, crack propagation during peel testing becomes more difficult, leading to higher measured peeling forces compared to EPDM-based systems.

For the epoxy-based adhesives GC6 and GC11, the situation is different. In many cases, the tested samples exhibit failure mode FM5, meaning that rupture occurs within the gasket before stable interfacial debonding can be established. Under these conditions, the measured peeling force no longer corresponds directly to the true interfacial bond strength, but rather provides only a lower limit for it. The higher forces observed in NBR-based systems are therefore mainly related to the mechanical behaviour of the gasket itself. Since NBR gaskets generally fail at higher loads, they naturally produce higher measured force levels than EPDM under FM5 conditions. Consequently, the superior apparent performance of NBR in these systems does not necessarily imply a stronger adhesive interface, but rather reflects the higher lower-limit force associated with gasket rupture.

Another aspect worth discussing is the difference between the various parameters presented in Table 4: the peeling force (F_c), the critical energy release rates (G_c and $G_{c,\text{elastic}}$), and the parameters directly provided by the Zwick Roell software (F_{max} and F_{av}). Until now, adhesive performance at Alfa Laval had mainly been evaluated using F_{max} and F_{av}. However, these parameters provide a simplified description of the peel process, as they do not explicitly account for important physical aspects such as stable crack propagation, gasket geometry or the elastic energy dissipated through deformation of the elastomeric substrate.

The parameter F_{av} provides a reasonable approximation for weak adhesive systems such as GC5 or even GC8, where debonding initiates almost immediately and the entire curve is dominated by interfacial crack propagation. However, it systematically underestimates the performance of stronger adhesives such as GC6 and GC11, where a significant portion of the applied energy is consumed by elastic deformation or gasket rupture rather than stable interfacial peeling. Conversely, F_{max} tends to overestimate the adhesion performance of weak systems, since local force peaks are not representative of the overall crack propagation process. Nevertheless, for systems dominated by failure mode FM5, where gasket rupture occurs before stable peeling can be established, F_{max} progressively becomes a more representative estimator of the effective adhesion performance.

In contrast, the critical peeling force F_c provides a more physically meaningful description of the peel process, as it specifically characterizes the force associated with stable crack propagation along the interface. Although its determination involves a certain degree of subjectivity due to the selection of the peeling interval, it offers a significantly more representative measure of the actual adhesion performance. This behaviour is clearly illustrated in Figure 19, where F_{max} and F_{av} are plotted as a function of F_c. Data points located close to the reference line $F = F_c$ indicate good agreement with the calculated critical force, whereas large deviations reveal poor estimations of the true adhesive performance.

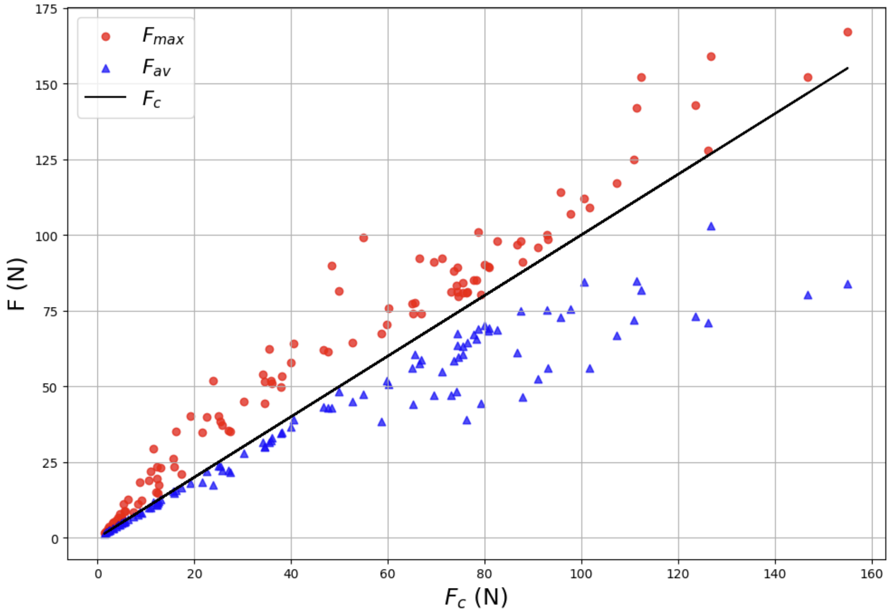

Figure 19: Comparison between the software-derived parameters (F_{max} and F_{av}) and the calculated critical peeling force F_c. The solid line represents the ideal relation $F = F_c$, indicating where is the accurate estimation of the effective peeling force.

The energy release rate parameters, G_c and $G_{c,\text{elastic}}$, provide an additional advantage, as they characterize the adhesion performance independently of the gasket width. In other words, these parameters describe the behaviour of the gasket–adhesive–metal system independently of its geometric dimensions. This aspect is particularly relevant in the context of gasketed plate heat exchangers, where gasket width may vary substantially depending on the size and design of the equipment. Consequently, the energy-based parameters enable comparisons and predictions across systems with different gasket geometries, something that the critical force F_c alone cannot achieve. The differences observed between G_c and $G_{c,\text{elastic}}$ are shown in Figure 20 and are consistent with the expected physical behaviour of the systems.

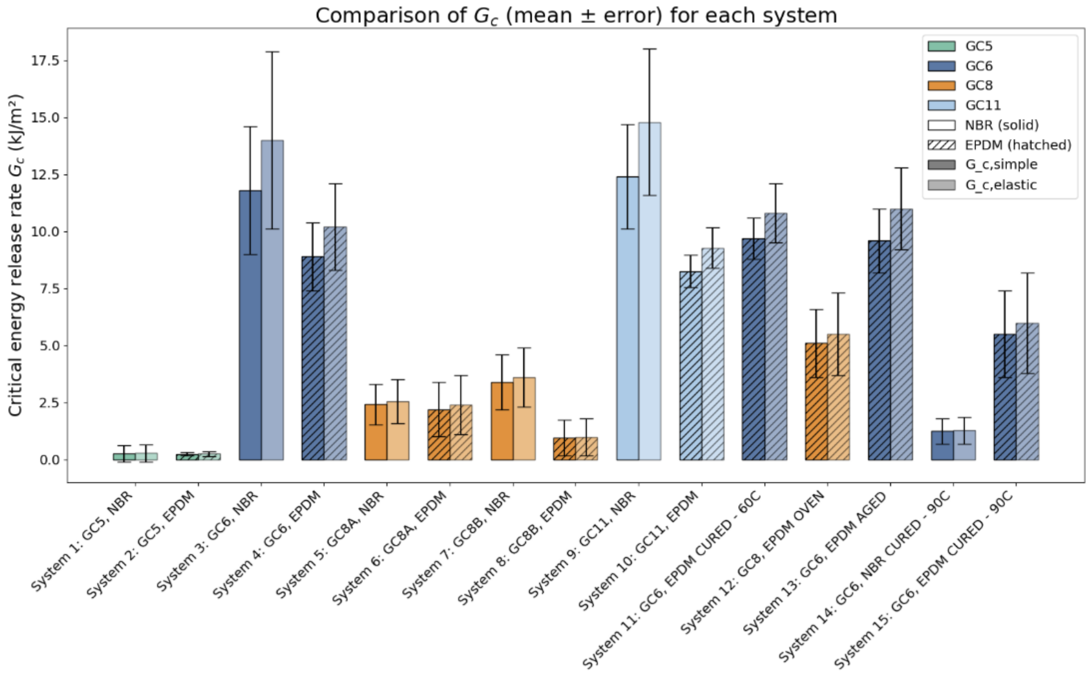

Figure 20: Critical energy release rate (G_c) of each gasket-adhesive system computed using the simple model (Equation (14)) and the taking into account the elastic contribution (Equation (11)). In addition, it is included the mean, error and individual points of each system.

For weak adhesive systems such as GC5, the simple model provides results very similar to those obtained when the elastic contribution is included, indicating that the energy dissipated through gasket deformation is relatively small. However, for systems with moderate or high bond strength, such as GC6, GC8 and GC11, a significant fraction of the supplied energy is consumed in elongating and deforming the elastomeric gasket during peeling. Under these conditions, the simple model substantially underestimates the actual energy released during crack propagation. As a result, larger differences are observed between G_c and $G_{c,\text{elastic}}$ as the bond strength increases. The elastic contribution can therefore not be considered negligible. On the contrary, it represents an essential component for a complete and physically consistent description of the peeling phenomenon in elastomeric bonded systems.

9.3 Water jetting

Water jet cleaning experiments were carried out in order to evaluate the serviceability of the adhesively bonded gasket systems under realistic cleaning conditions representing industrial maintenance procedures used in gasketed plate heat exchangers. Unlike peel testing, whose primary purpose is to characterize the intrinsic adhesion performance of the bonded interface under controlled mechanical loading, water jetting introduces a more complex loading scenario involving localized hydrodynamic forces and a progressive crack initiation at the interface. The cleaning experiments were performed using a Kärcher Professional HD 10/21-4 S operating at a pressure of 210 bar. Cleaning was carried out using a rotary nozzle configuration with water at a temperature of approximately $30°C$. The selected cleaning parameters were chosen in order to balance effective fouling removal with the need to evaluate the potential degradation and detachment of the adhesive joints.

The same gasket samples described in Section 9.1 were employed for the water jetting experiments. This approach allows the cleaning process of real GPHEs to be realistically emulated while simultaneously maintaining the same geometry to that used in peel testing experiments. As a result, a reliable comparison between peel testing performance and cleaning resistance can be established. In order to perform the water jetting experiments in a controlled and repeatable manner, a special fixture was designed and manufactured, as shown in Figure 21. This fixture allowed the samples to be securely positioned while ensuring a consistent exposure during spraying.

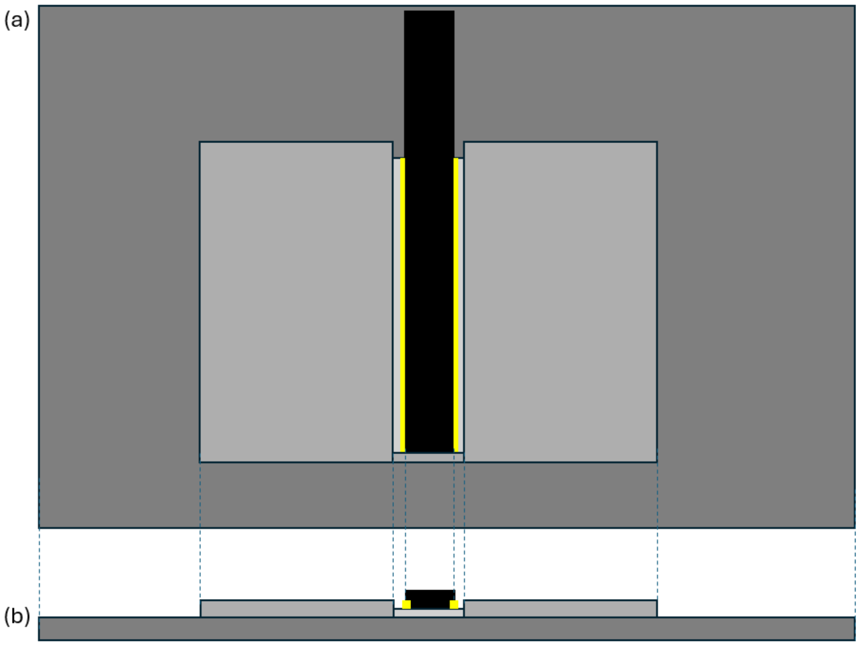

Figure 21: (a) Bird's-eye view and (b) front view diagram of the fixture used for water jetting. Samples composed by a plate (in light gray) bonded to a gasket (in black) using an adhesive (in yellow) are secured by a metal fixture (in dark gray) while is being sprayed during the water jetting cleaning.

The experimental procedure consisted of inserting the bonded samples into the fixture and positioning the nozzle at an approximate stand-off distance of 5 cm from the sample surface. Water spraying was then initiated while progressively varying the spraying angle from approximately 90° to 30° relative to the surface. Under these conditions, weak adhesive systems typically detached almost immediately upon exposure to the water jet at 90°. Systems with intermediate adhesion strength generally required lower spraying angles before debonding occurred, whereas the strongest adhesive systems remained attached independently of spraying angle and exposure time. Table 5 summarizes the water jetting results obtained for the different gasket–adhesive systems, including whether peel-off occurred, the spraying angle at which debonding happened and the corresponding failure mode observed. Systems are displayed in the table ranked from highest to lowest according to the critical force F_c obtained during peel testing:

# System	Peel-off	Peel-off angle	FM	F_c (N)
System 9: GC11 + NBR	No	-	-	109 ± 21
System 3: GC6 + NBR	No	-	-	104 ± 25
System 13: GC6 + EPDM (*)	Yes / No	-	-	84 ± 12
System 11: GC6 + EPDM (**)	No	-	-	83.9 ± 8.3
System 4: GC6 + EPDM	No	-	-	79 ± 14
System 10: GC11 + EPDM	No	-	-	72.6 ± 6.3
System 15: GC6 + EPDM (***)	Yes	30°	3	48 ± 17
System 12: GC8A + EPDM (****)	Yes	30°	3	45 ± 13
System 7: GC8B + NBR	Yes	45°	3	30 ± 10
System 5: GC8A + NBR	Yes	60°	3	21.3 ± 7.8
System 6: GC8A + EPDM	Yes	90°	3	20 ± 11
System 14: GC6 + NBR (***)	Yes	90°	3	10.9 ± 5
System 8: GC8B + EPDM	Yes	90°	3	8.4 ± 6.9
System 1: GC5 + NBR	Yes	90°	1	2.4 ± 3.2
System 2: GC5 + EPDM	Yes	90°	1	2.14 ± 0.65

Table 5: Water jetting results of all the tested systems ranked from highest to lowest according to the critical force F_c. It is shown whether peel-off occurred, the spraying angle at which debonding happened, the failure mode observed and their corresponding critical force. The symbols denote specific sample conditions: (*) aged sample, (**) curing temperature $60°C$ below recommendations, (***) curing temperature $90°C$ below recommendations, and (****) oven-cured sample instead of room-temperature curing.

These results confirm a clear correlation between peel testing performance and the behaviour observed during water jetting experiments. The ranking of the adhesive systems based on the critical force obtained from peel testing is in strong agreement with the detachment behaviour observed under high-pressure water jetting conditions. The weakest adhesive systems, based on GC5, detach easily even at a spraying angle of 90°. As the bond strength increases, progressively steeper spraying angles are required to achieve gasket detachment. This trend ultimately reaches a limit in the case of the System 10 (GC11 + EPDM), for which no detachment was observed under the investigated cleaning conditions. In this sense, the corresponding critical force, $72.6 \pm 6.3, \mathrm{N}$, represents the lowest experimentally observed value for which complete survival during water jetting was achieved. This value can therefore be interpreted as an experimentally determined operational threshold for gasket serviceability under the present cleaning conditions.

Nevertheless, a partial anomaly is observed for System 13, where some samples survived the water jetting process while others detached. This behaviour is most likely associated with the statistical nature of the ageing process. As discussed previously, the majority of aged samples exhibit critical forces comparable to those that had not been aged (System 4), indicating that the ageing conditions were not sufficiently severe to significantly degrade the interface in most cases. However, localized variations may still occur due to the stochastic nature of moisture diffusion and interfacial degradation processes. The samples that detached during water jetting (2 out of 4) likely exhibited locally reduced interfacial strength, where water molecules had penetrated the adhesive–gasket interface and promoted weaker intermolecular interactions and easier crack propagation. Apart from this particular case, all other systems behaved consistently with the expected trend derived from peel testing.

The observed failure modes during water jetting also deserve attention, as they differ in several cases from those obtained during peel testing. This suggests that the loading conditions introduced by high-pressure water jetting promoted different failure mechanisms at the interface. In particular, exposure to water appears to weaken the adhesive joint and promote adhesive failure either at the metal interface (FM1) or at the gasket interface (FM3). Interestingly, failure mode FM5 was never observed during water jetting experiments, which suggests that, under the investigated conditions, the water jetting process does not generate stresses sufficiently high to mechanically rupture the gasket material itself, but instead promotes progressive weakening and debonding of the adhesive interface.

9.4 SEM-EDS

In order to further investigate the anomalous behaviour observed for System 13 during the water jetting experiments, the metallic surface of one of the detached samples was analyzed using Scanning Electron Microscopy coupled with Energy-Dispersive X-ray Spectroscopy (SEM-EDS). Although visual inspection after water jetting initially suggested a pure FM1 failure mode, higher magnification SEM observations revealed the presence of small EPDM fragments still attached to the metallic surface, indicating that the failure mode actually corresponds to a combination of FM1 and FM4, a behaviour that was not observed in any of the peel testing samples. These features are shown in Figure 22.

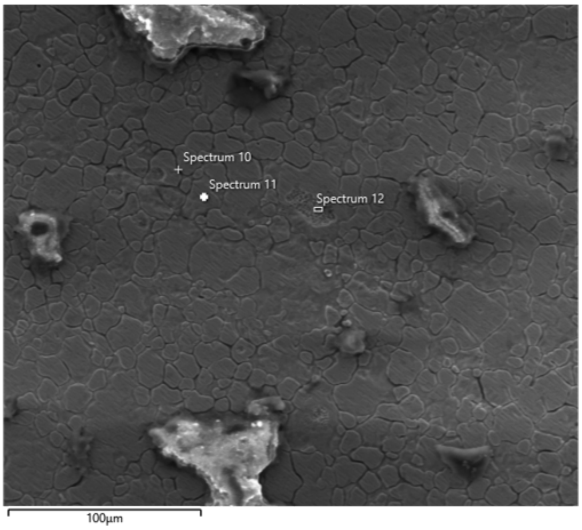

Figure 22: SEM image performed on the metallic surface of one of the detached samples of System 13 (GC6 + EPDM aged) used during water jetting. It confirms the presence of small EPDM fragments still attached to the metallic surface.

The coexistence of FM1 and FM4 suggests that in this case, contrary to other samples that did not detached during water jetting or the samples that were evaluated with peel testing, the ageing treatment was effective in degrading the adhesive interface. The regions that exhibit FM1, water molecules likely penetrated through the adhesive interface during the ageing process, progressively weakening the interfacial bonding strength. Most probably, moisture diffusion reached the adhesive–metal interface and reduced the intermolecular interactions and chemical bonding that helped the adhesion. As a consequence, the crack propagation energy required for debonding during water jetting is lowered. In contrast, the regions where EPDM fragments remained attached to the metallic surface (FM4) indicate that moisture penetration was not complete and preserved an strong adhesive bond, causing micro-scale rupture within the gasket material itself during the detachment caused by water jetting. This local behaviour is the one that have been seen during peel testing (there was a dominance of FM4) and likely for the samples that did not detached during water jetting. Therefore the anomaly found in Table 5 could be attributed to an statistical behaviour of the ageing process, in some samples it has an impact and in other it does not.

In addition to the remaining gasket fragments, the SEM image also revealed the characteristic grain boundary structure of the stainless steel substrate. Due to the high contrast observed between grains and grain boundaries, EDS analyses were performed in both regions in order to investigate possible compositional differences. The spectrum acquired on the grain interiors shown in Figure 23b (Spectrum 11) mainly exhibited peaks corresponding to Fe (64.1%), Cr (15.5%) and Ni (9.7%), which are the principal alloying elements of stainless steel, together with a relatively small carbon contribution (7.0% of C) likely associated with residual adhesive or gasket material.

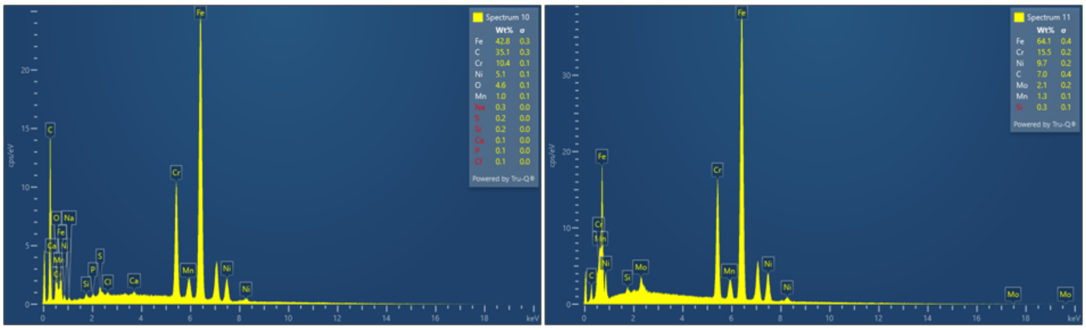

(a) Spectrum 10

(b) Spectrum 11

Figure 23: Spectroscopy performed on top of grains boundaries (a) and on top of grains (b).

However, the spectrum obtained directly on the grain boundaries shown in Figure 23a (Spectrum 10) revealed a significantly different composition: Fe (42.8%), C (35.1%), Cr (10.4%), Ni (5.1%) and O (4.6%). The substantial increase in carbon content together with the presence of oxygen is the main difference. Although this increase in the peak of carbon may be caused by chromium carbides since they naturally segregate at grain boundaries in stainless steels, [33] it is discarded considering the simultaneous reduction in chromium intensity and the unusually high carbon concentration. The results instead suggest the presence of residual adhesive material that remains anchored within the grain boundary regions. Since the adhesive is initially applied in liquid form prior to curing, it is plausible that it penetrated locally into surface irregularities and microscopic grain boundary grooves of the stainless steel substrate. This behaviour indicates a good wettability of the GC6 adhesive on the metallic surface and demonstrates the existence of mechanical interlocking as a contributing adhesion mechanism. Therefore, the penetration of the adhesive into these microscopic surface features may explain the good performance seen in samples with the GC6 adhesive.

10 Conclusion

This thesis has investigated the serviceability of adhesively bonded gaskets used in gasketed plate heat exchangers under cleaning conditions representative of industrial high-pressure water jetting. In collaboration with Alfa Laval, different gasket–adhesive systems based on NBR and EPDM elastomers together with several industrial adhesives, ranging from weak silicone-based systems to high-performance epoxy adhesives, were experimentally characterized and compared.

The theoretical framework presented throughout this work established the fundamental concepts governing adhesion, including interfacial adhesion mechanisms, crosslinking phenomena, elastomer behaviour, peel testing mechanics, failure mode possibilities and the influence of cleaning parameters during water jetting. Particular attention was devoted to understanding the mechanics of crack propagation at the interface gasket-metal, leading to the conclusion that three main parameters define it: the critical peeling force (F_c) and the critical energy release rates (G_c and $G_{c,\text{elastic}}$)

Experimentally, peel testing proved to be an effective method for quantifying the adhesion performance of the investigated systems. Different approaches for evaluating bond strength were analyzed and compared, including the software-derived parameters F_{max} and F_{av}, the critical peeling force F_c and the critical energy release rates G_c and $G_{c,\text{elastic}}$. The results demonstrate that F_c provides a significantly more representative description of the actual peeling process in comparison to the software-derived parameters since it specifically characterizes the force associated with stable crack propagation along the interface. In addition, energy-based parameters G_c and $G_{c,\text{elastic}}$ offer the advantage of describing adhesion independently of gasket geometry, making them particularly useful for the prediction of the bond strength of gaskets with different dimensions. The comparison between G_c and $G_{c,\text{elastic}}$ also confirmed the importance of considering the elastic contribution of the gasket, especially for high-strength adhesive systems where a substantial fraction of the applied energy is dissipated through elastomer deformation.

The experimental results further revealed significant differences in performance between the investigated adhesives. Weak adhesive systems such as GC5 exhibited poor interfacial adhesion and detached easily during water jetting, whereas epoxy-based systems such as GC6 and GC11 achieved remarkably high bond strengths and favorable failure modes, where the gasket itself became the limiting factor of the assembly. The importance of curing conditions was also demonstrated, particularly for epoxy-based systems, where insufficient curing temperatures resulted in reduced crosslink density and degraded adhesion performance. Moreover, the chemical compatibility between adhesive and gasket material was shown to play a major role, especially for nitrile-based adhesive systems interacting with NBR gaskets.

One of the main outcomes of this work is the clear correlation identified between peel testing performance and gasket serviceability under water jetting conditions. The results demonstrate that the resistance of the bonded systems to high-pressure cleaning is directly related to the measured critical peeling force. Systems with $F_c < 21.3, \mathrm{N}$ failed even at a spraying angle of 90°, indicating very poor serviceability. Systems with intermediate adhesion strength, approximately within the range $21.3, \mathrm{N} < F_c < 72.6, \mathrm{N}$, detached only at intermediate spraying angles between 30° and 60°. Finally, systems with $F_c > 72.6, \mathrm{N}$ survived the investigated water jetting conditions without gasket detachment. Therefore, these experimentally determined values establish practical limits for the cleaning conditions under which adhesively bonded gaskets can safely operate. They provide a simple criterion to evaluate gasket serviceability during high-pressure water jetting and help define cleaning conditions that avoid unwanted gasket detachment during maintenance.

Additional insight into interfacial degradation mechanisms was obtained through SEM-EDS analysis of an aged sample. The results suggest that moisture penetration during ageing can locally weaken the adhesive interface, promoting adhesive failure during water jetting while preserving strong adhesion in other regions. However, this ageing process did not behave in the same way for all samples, suggesting that it is a statistical process involving a degree of randomness. Furthermore, microscopic observations confirmed the presence of wetting and mechanical interlocking as adhesion mechanisms that contribute to the bonding between the adhesive and the stainless steel substrate.

Overall, the results obtained in this thesis confirm that peel testing and water jetting are strongly correlated and together provide a complete description of the serviceability of adhesively bonded plate heat exchanger gaskets. The methodology developed in this work therefore represents a valuable framework for evaluating and optimizing industrial adhesive systems for GPHE applications.

Finally, several directions for future work can be proposed. A more extensive investigation of ageing phenomena and moisture diffusion mechanisms would help to better understand the long-term degradation of adhesive interfaces. In addition, a more accurate determination of the real bonded area between gasket and metal would improve the calculation of the critical energy release rate G_c. In this work, the base gasket width ($w = 8.78, \mathrm{mm}$) was assumed to represent the bonded width. Although this approximation is reasonably close to reality, the actual bonded area changes during curing due to gasket compression and adhesive spreading. Further efforts should also focus on developing experimental procedures that provide more reproducible sample behaviour, thereby reducing the statistical variability commonly observed in polymeric bonded systems.

References

[1] Alfa Laval, *The Theory Behind Heat Transfer*, 2025. [Online]. Available: `https://www.alfalaval.com/globalassets/documents/microsites/heating-and-cooling-hub/alfa_laval_heating_and_cooling_hub_the_theory_behind_heat_transfer.pdf`.

[2] Alfa Laval, “Gasketed plate-and-frame heat exchangers,” 2026. [Online]. Available: `https://www.alfalaval.com/products/heat-transfer/plate-heat-exchangers/gasketed-plate-and-frame-heat-exchangers/`.

[3] F. C. C. Galeazzo, R. Y. Miura, J. A. W. Gut, and C. C. Tadini, “Experimental and numerical heat transfer in a plate heat exchanger,” *Chemical Engineering Science*, vol. 61, no. 21, pp. 7133–7138, 2006.

[4] Alfa Laval, “Alfa laval digital asset library,” 2026. [Online image repository]. Available: `https://dal.alfalaval.com/portal/#search-nr300-tree=6089`.

[5] K. Xu and R. Smith, “Design and optimization of plate heat exchanger networks,” in *13th International Symposium on Process Systems Engineering (PSE 2018)*, vol. 44 of *Computer Aided Chemical Engineering*, pp. 451–456, Elsevier, 2018.

[6] Alfa Laval, “Gphe selection guide,” 2026. [Online]. Available: `https://www.alfalaval.com/microsites/gphe/tools/selectionguide/`.

[7] Alfa Laval, “Brazed plate heat exchangers,” 2026. [Online]. Available: `https://www.alfalaval.com/products/heat-transfer/plate-heat-exchangers/Brazed-plate-heat-exchangers/`.

[8] Alfa Laval, “Cleaning services for gasketed plate heat exchangers,” 2026. [Online]. Available: `https://www.alfalaval.com/microsites/gphe/services/cleaning/`.

[9] J. Comyn, “What are adhesives and sealants and how do they work?,” in *Adhesive Bonding*, pp. 41–78, Elsevier, 2021.

[10] S. Wu, *Polymer Interface and Adhesion.* New York: Marcel Dekker, 1982.

[11] J. C. Hernández-Ortiz and E. Vivaldo-Lima, “Crosslinking,” in *Handbook of Polymer Synthesis, Characterization, and Processing* (E. S. Guerra and E. Vivaldo-Lima, eds.), ch. 9, John Wiley & Sons, 2013.

[12] Alfa Laval, “Gluing instruction for gc5,” tech. rep., Alfa Laval, 2024. Internal document, not publicly available.

[13] Alfa Laval, “Gluing instruction for gc6,” tech. rep., Alfa Laval, 2024. Internal document, not publicly available.

[14] Alfa Laval, “Gluing instruction for gc8,” tech. rep., Alfa Laval, 2021. Internal document, not publicly available.

[15] Alfa Laval, “Gluing instruction for gc11,” tech. rep., Alfa Laval, 2021. Internal document, not publicly available.

[16] J. Sadowski, “Debonding of adhesively bonded rubber gaskets from metal plates through immersion in liquid nitrogen,” Master’s thesis, Lund University, 2025.

[17] S. Ebnesajjad, “Introduction and adhesion theories,” in *Handbook of Adhesives and Surface Preparation*, pp. 3–13, Elsevier, 2011.

[18] E. A. S. Marques and L. F. M. da Silva, “Theory of adhesion,” in *Structural Adhesive Bonding for Automotive Applications*, pp. 15–23, Elsevier, 2026.

[19] W. C. Wake, “Theories of adhesion and uses of adhesives: A review,” *Polymer*, vol. 19, no. 3, pp. 291–308, 1978.

[20] V. Kovacevic, “Surface and interface phenomenon in polymers,” in *International Workshop on Advanced Polymer Science and Turbulent Drag Reduction*, (The Abdus Salam International Centre for Theoretical Physics, Trieste, Italy), 2008. [Online]. Available: `https://indico.ictp.it/event/a07182/session/49/contribution/29/material/0/0.pdf`.

[21] I. M. Alarifi, “A comprehensive review on advancements of elastomers for engineering applications,” *Advanced Industrial and Engineering Polymer Research*, vol. 6, no. 4, pp. 451–464, 2023.

[22] E. L. de Souza, M. de Sousa Zanzi, K. V. de Paiva, J. L. G. Oliveira, G. M. de Oliveira Barra, and G. B. Dutra, “Experimental and numerical analyses of thermo-oxidative aging in nbr and epdm rubber with different lengths,” *Polymer*, vol. 334, p. 128694, 2025.

[23] Alfa Laval, “Nitrile rubber, performance - nbr-p for phe gaskets,” tech. rep., Alfa Laval, 2022. Internal document, not publicly available.

[24] Alfa Laval, “Ethylene-propylene diene rubber (epdm),” tech. rep., Alfa Laval, 2023. Internal document, not publicly available.

[25] Alfa Laval, “Gasket solutions for semiconductor applications,” 2024. [Online]. Available: `https://www.alfagaskets.com/Gasket-solutions-for-semicon.pdf`.

[26] Alfa Laval, “Instruction for curing tightening dimensions for heat plate exchanger plates,” tech. rep., Alfa Laval, 2024. Internal document, not publicly available.

[27] M. D. Bartlett, S. W. Case, A. J. Kinloch, and D. A. Dillard, “Peel tests for quantifying adhesion and toughness: A review,” *Progress in Materials Science*, vol. 137, p. 101086, 2023.

[28] M. Rezaee, L.-C. Tsai, M. I. Haider, *et al.*, “Quantitative peel test for thin films/layers based on a coupled parametric and statistical study,” *Scientific Reports*, vol. 9, p. 19805, 2019.

[29] Alfa Laval, “Adhesive for bonded gaskets to metal plate heat exchangers,” tech. rep., Alfa Laval, 2025. Internal document, not publicly available.

[30] Alfa Laval, “High pressure water jet of tl35-b freshly glued,” tech. rep., Alfa Laval, 2026. Internal concept report, not publicly available.

[31] A. Kale, S. K. Singh, N. Sateesh, and R. Subbiah, “A review on abrasive water jet machining process and its process parameters,” *Materials Today: Proceedings*, vol. 26, pp. 1032–1036, 2020.

[32] Kärcher, *Expert Guide for Professional Pressure Washers*, 2025. [Online]. Available: `https://s1.kaercher-media.com/media/file/226527/expertguide-fo-r-proffsen-ho-gtrycktva-tt.pdf`.

[33] Elsevier, “Grain boundary carbide,” 2026. [Online]. Available: `https://www.sciencedirect.com/topics/engineering/grain-boundary-carbide`.